

Contribution of the long non-coding RNA H19 to neonatal and adult rodent β -cell mass expansion

Running title: Role of H19 in β -cell mass expansion

Clara Sanchez-Parra¹, Cécile Jacovetti¹, Olivier Dumortier², Kailun Lee³, Marie-Line Peyot⁴, Claudiane Guay¹, Marc Prentki⁴, D. Ross Laybutt³, Emmanuel Van Obberghen^{5,6} and Romano Regazzi¹

1. Department of Fundamental Neurosciences, University of Lausanne, Switzerland
2. University Côte d'Azur, INSERM, CNRS, IRCAN, France
3. Diabetes and Metabolism Division, Garvan Institute of Medical Research, Darlinghurst, Sydney, New South Wales, Australia
4. Montreal Diabetes Research Center and Centre de Recherche du CHUM, Montréal, Québec, Canada
5. University Côte d'Azur, CHU, INSERM, CNRS, IRCAN, France
6. University Côte d'Azur, CHU, CNRS, L2PM, France (present address)

Correspondence to:

Dr. Romano Regazzi, Department of Fundamental Neurosciences

Rue du Bugnon 9, CH-1005 Lausanne, Switzerland

Tel. : +41 21 692 52 80 / Fax : +41 21 692 52 55

E-mail: Romano.Regazzi@unil.ch

ABSTRACT

Pancreatic β -cell expansion throughout the neonatal period is essential to generate the appropriate mass of insulin-secreting cells to maintain blood glucose homeostasis later in life. Hence, defects in this process can predispose to diabetes development at adulthood. Global profiling of the transcripts in pancreatic islets of newborn and adult rats revealed that the expression of the long non-coding RNA H19 is controlled by the transcription factor E2F1 and is profoundly downregulated during the post-natal period. H19 silencing decreased newborn β -cell expansion while its re-expression promoted proliferation of adult β -cells via a mechanism involving the microRNA let-7 and the activation of Akt. The offspring of rats kept on a low protein diet during gestation and lactation display a reduced β -cell mass and an increased risk to develop diabetes at adulthood. We found that the islets of newborn rats born from dams on a low protein diet express lower levels of H19. Moreover, we observed that H19 expression raises in the islets of obese mice under conditions of increased insulin demand. Taken together, our data suggest that the lncRNA H19 plays an important role in postnatal rat β -cell mass expansion and contributes to the mechanisms compensating for insulin resistance under obesity conditions.

INTRODUCTION

Pancreatic β -cells, located within the islets of Langerhans, maintain blood glucose levels in a physiologically relevant range by precisely adapting insulin secretion to circulating levels of nutrients, particularly glucose (1). Insulin-secreting cells acquire a fully differentiated phenotype only after birth. Before weaning neonatal β -cells produce and release insulin in response to amino acids but the capacity to secrete insulin in response to a rise in glucose levels, a characteristic feature of fully mature β -cells, is still missing (2; 3).

Another hallmark of newborn β -cells is a strong proliferative capacity that allows a massive expansion of the number of insulin-secreting cells during the postnatal period. After weaning, the replication slows down to maintain a more or less constant β -cell mass during the entire life (4). Defective β -cell expansion early in life can result in an insufficient mass of insulin-secreting cells at adulthood, predisposing the individuals to the development of diabetes. Under conditions associated with increased metabolic demands, such as pregnancy and obesity, β -cells raise their secretory activity and their replication rate. Failure to compensate for insulin-resistance linked to pregnancy or obesity can lead to hyperglycemia and eventually to the onset of gestational or type 2 diabetes, respectively (5).

So far, most studies investigating the mechanisms driving postnatal β -cell maturation focused on protein-coding genes. However, the advent of high throughput RNA sequencing revealed that most genome sequences generate RNA molecules which are not coding for proteins (6). We now know that the non-coding transcriptome is involved in multiple biological processes influencing development, differentiation and metabolism (7-9). Emerging evidence points to a role for non-coding RNAs also in postnatal β -cell maturation. Indeed, we showed that the nutritional shift at weaning from a fat-rich mother milk to a carbohydrate-rich chow diet triggers vast changes in the microRNA (miRNA) profile of newborn β -cells that are instrumental for the acquisition of glucose responsiveness and of a mature secretory phenotype (10).

Beside small non-coding RNAs, the mammalian transcriptome includes a large number of long non-coding RNAs (lncRNAs) containing more than 200 nucleotides (11-13). Recently, thousands of lncRNAs were identified in human and mouse pancreatic islets (14-16). Many of these lncRNAs are specifically expressed in islets and are induced during β -cell differentiation. These

findings suggest a role for lncRNAs in developmental programming, proper functioning and/or maintenance of pancreatic islet cells.

The aim of this project was to identify lncRNA-based mechanisms that contribute to the acquisition of the mature β -cell phenotype and that control the size of the functional β -cell mass. Screening for lncRNAs differentially expressed during islet postnatal maturation revealed the downregulation of H19, a maternally imprinted intergenic lncRNA generated from the *Igf2* locus (17). We provide evidence indicating that H19 contributes to β -cell mass expansion in newborn rats and is re-expressed in adult islets under conditions of increased insulin demand. Moreover, we show that the level of H19 is lower in the islets of pups born from dams kept on a low protein diet during gestation and lactation, and which display a reduced β -cell mass and increased risk to develop diabetes at adulthood. Our findings provide new insights into the role of H19 in newborn and adult rodent β -cells and unveil a potential mechanism explaining the increased diabetes susceptibility of the offspring of mothers kept on deleterious dietary conditions during pregnancy and lactation.

RESEARCH DESIGN AND METHODS

Chemicals

IL-1 β , hexadimethrine bromide, histopaque 1119 and 1077 were obtained from Sigma-Aldrich (St. Louis, MO). 3-isobutyl-1-methylxanthine (IBMX) was purchased from Merck (Whitehouse Station, NJ, USA), IFN- γ from R & D Systems (Minneapolis, MN, USA) and TNF- α from Enzo Life Sciences (Farmingdale, NY, USA).

Animals

Three month old male Sprague Dawley rats were purchased from Janvier Laboratories (Le Genest-Saint-Isle, France). P1 to P31 pups were obtained by collecting the offspring of pregnant Sprague Dawley rats. Pregnant Wistar rats were fed during gestation and lactation with a control diet (20% [w/w] protein) or an isocaloric low protein diet (8% [w/w] protein) (Hope Farm, Woerden, the Netherlands) (18). 13-16 week old C57BL/KsJ db/db and C57BL/6J ob/ob mice and age-matched lean control mice (db/+ C57BL/KsJ or -/- C57BL/6J, respectively) were taken from the Garvan Institute breeding colonies. 5-week old C57BL/6 male mice (Charles River Laboratories, Raleigh, NC, USA) were fed with a normal (ND) or a high-fat diet (HFD) for 8 weeks (Bioserv F-3282, 60% energy from fat, Frenchtown, NJ, USA). The mice that after 7.5 weeks on HFD weighed between 33 and 39 g were classified as low responders (LDR), while those weighing between 39 and 45 g were defined as high responders (HDR). Weight, glycemia and insulinemia of these animals were reported previously (19).

Microarray profiling

RNA was isolated from pools of islets of 5 P10 pups from 3 different mothers and 3 individual adult rats. mRNA and lncRNA profiling using the Rat lncRNA Array v2.0 and data analysis were carried out by Arraystar (Rockville, MD, USA). Differentially expressed transcripts were identified through Volcano Plot filtering (fold change ≥ 2 , nominal $p \leq 0.05$). The data are available on the GSE106919 record using the secure token: qfolagkublsfrov.

Culture of INS832/13 and 1.1B4 cells

The rat β -cell line, INS832/13 was kindly provided by Dr. C. Newgard (Duke University, USA) and was cultured as described (20). The cells were seeded at a density of $4 \times 10^4/\text{cm}^2$ for immunocytochemistry and cell death assessment, at $7.5 \times 10^4/\text{cm}^2$ for insulin secretion and $1.1 \times 10^5/\text{cm}^2$ for RNA isolation. The human β -cell line 1.1B4 was generously provided by Dr. P. Flatt (University of Ulster) and was cultured as described (21).

Isolation and culture of islet cells

Rat pancreatic islets were isolated by collagenase digestion (22), purified on a Histopaque density gradient and then cultured as described (10). Islet cells were dissociated by trypsinization and seeded at a density of $5 \times 10^4/\text{cm}^2$ for immunocytochemistry and $10^5/\text{cm}^2$ for RNA isolation.

Fluorescence activated cell sorting

Dissociated islet cells from newborn and adult rats were sorted by FACS based on β -cell autofluorescence (23). Immunocytochemistry analysis using anti-insulin antibodies (#A0564, Dako, Basel, Switzerland) showed that $94 \pm 1\%$ of the cells in the purified fraction were insulin-positive.

Cell transfection

Overexpression was achieved by transfecting a pcDNA3 plasmid harboring the sequences of the lncRNA using Lipofectamine 2000TM (Invitrogen, Carlsbad, CA) in INS832/13 cells or Lipofectamine 3000TM (Invitrogen) in islet cells. Downregulation was obtained by transfecting siRNAs against GFP (Eurogentec, Seraing, Belgium), H19 (Thermo Fisher Scientific, Waltham, MA, USA), Ago2 or E2f1 (GE Healthcare Europe) or miRCURY LNATM microRNA Inhibitors (anti-miRs) (Exiqon, Bedvaek, Denmark) using Lipofectamine 2000TM (INS832/13 cells) or Lipofectamine RNAiMAXTM (Invitrogen) (islet cells).

RNA isolation and detection

RNA was isolated with the miRNeasy kit (Qiagen, Basel, Switzerland) for islet cells and with the ZR RNA MiniPrepTM kit (Zymo Research, Irvine, CA) for INS832/13 cells. The samples were treated with DNase (Promega, Madison, WI, USA) prior to retro-transcription using the M-MLV reverse transcriptase, RNase H minus (Promega). For quantification of lncRNAs and mRNAs,

Real-time PCR was performed using iQ SYBR Green mix. LncRNA and mRNA primers are provided in the supplemental table 1. For miRNA quantification, Real-time PCR was carried out using the miRCURY LNATM Universal RT microRNA PCR kit (Exiqon).

Immunocytochemistry

Glass coverslips were coated with poly-L-lysine alone for dissociated islet cells or together with laminin for INS832/13 cells. The cells were fixed with cold-methanol and permeabilized with PBS supplemented with 0.5% (v/v) saponin (Sigma-Aldrich). The coverslips were incubated in blocking buffer (PBS supplemented with 0.5% (v/v) saponin and 1% (w/v) BSA (Sigma-Aldrich)) and then exposed to primary antibodies at the following dilutions: 1:700 rabbit anti-Ki67 (#ab15580, Abcam, Cambridge, UK) and 1:500 guinea pig anti-insulin (#A0564, Dako). After washing, the coverslips were incubated with goat anti-rabbit Alexa-Fluor-488 or goat anti-guinea pig Alexa-Fluor-555, diluted at 1:500 (#A11008 and #A21435 respectively, ThermoFisher Scientific). Finally, they were incubated with Hoechst 33342 (Invitrogen), mounted on glass slides and visualized with a Zeiss Axiovision fluorescence microscope. For BrdU immunocytochemistry, the cells were incubated for 48h with BrdU (#ab142567, Abcam). After exposure to blocking buffer and prior exposure to mouse anti-BrdU antibody (1:400, #BD55627, BD Biosciences), DNA was denatured with 2N HCl. BrdU-positive cells were visualized with a goat anti-mouse Alexa-fluor-555 antibody (1:500; #A21422 ThermoFisher Scientific). Examples of Ki67 and BrdU positive cells are provided in Supplementary Fig.1. At least 1000 cells were analyzed for each condition.

Insulin secretion

Insulin secretion from INS832/13 cells was carried out as described previously (10).

Cell death assessment

INS832/13 cells were washed with PBS and incubated with Hoechst 33342 1 μ g/ml. The fraction of cells displaying pycnotic nuclei was scored after visualization under fluorescence microscopy (AxioCam MRc5, Zeiss). As a positive control for apoptosis, a fraction of cells were exposed during 24h to a combination of cytokines (TNF- α 10 ng/ml, IL-1 β 0.1 ng/ml, IFN- γ 30 ng/ml). About 500 cells were counted for each condition.

Protein extraction and western blotting

INS832/13 cells were washed in cold PBS and incubated for 15min in lysis buffer (20 mM Tris, pH 7.5, 2 mM EDTA and protease inhibitors (Roche)). The cells were then scraped, briefly sonicated and centrifuged to eliminate nuclei and cell debris. 30µg of proteins were loaded on acrylamide gels and transferred to polyvinylidene fluoride membranes. The membranes were placed for 1h in blocking buffer (0.1% (v/v) Tween 20 and 5% (w/v) BSA followed by overnight incubation at 4°C with primary antibodies diluted in blocking buffer. The antibodies used were the following: Rabbit anti-phospho-Akt, 1:500 (Thr308 (#9275S) or Ser473 (#4060S), Cell Signaling, Danvers, MA, USA); mouse anti-Akt, 1:500 (#2920, Cell Signaling); mouse anti-actin α , 1:15000 (#MAB1501, Merck & Cie, Schaffhausen, Switzerland). After one hour exposure at room temperature to horseradish peroxidase-coupled secondary antibodies, 1:15000, (Anti-Rabbit IgG (#111-165-144) and anti-mouse IgG (#111-165-166), Jackson ImmunoResearch Europe Ltd., Suffolk, UK) immunoreactive bands were visualized by chemiluminescence (ThermoFisher Scientific) using the ImageQXSuant LAS-4000 System.

Luciferase assay

The luciferase construct with eight *let-7* target sites in the 3'UTR of the *Renilla* gene was a gift from Yukihide Tomari (psiCHECK2-*let-7* 8x; Addgene plasmid # 20931). Luciferase activity was measured using a dual luciferase reporter assay (Promega, Madison, WI, USA) and was normalized to the *Firefly* activity generated by the same plasmid.

Statistical analysis

Data are means \pm SEM. Statistical significance was tested by unpaired or one sample Student's *t* test when two sets of data were analyzed and by one-way ANOVA followed by multiple comparison tests (Dunnet's or Tukey's) or Kruskal-Wallis with multiple comparison test (Dunn), when the experiments included more than two groups. H19 expression and phenotypic characteristics of the mice were correlated by linear regression, using F-test (Graphpad statistical package, La Jolla, CA).

RESULTS

To assess the contribution of lncRNAs to the acquisition of a fully differentiated β -cell phenotype, we used a microarray to search for lncRNAs differentially expressed between adult and neonatal rat islets (ten days after birth, P10). The array includes 5496 lncRNAs, 896 of which were upregulated and 1018 downregulated during islet maturation (fold change ≥ 2 ; nominal p-value ≤ 0.05) (GSE106919, Fig.1a). We decided to investigate in more detail the role of lncRNAs displaying the largest expression changes and, to avoid possible interferences from protein-coding genes, we focused exclusively on intergenic lncRNAs. Interestingly, the expression of H19 (NR_027324), a lncRNA generated from a maternally imprinted locus, was 303 times lower in the islets of adult compared to those of newborn rats (Fig.1b). These findings were confirmed by RT-PCR in whole islets (Fig.1c) and in FACS-purified β -cells (Fig.1d). A time course spanning the postnatal period showed that the expression of H19 is highest between P1 and P5 and strongly decreases thereafter (Fig.1e).

Several transcription factors can regulate the expression of H19. The level of one of these, E2F1, is reduced both in islets (Fig.1c) and purified β -cell (Fig.1d) upon postnatal maturation and displays an expression pattern that follows that of H19 (Fig.1e). Silencing of E2F1 in P10 islets (Supplementary Fig.2a) resulted in the downregulation of H19 (Fig.1f), suggesting that this transcription factor contributes to the control of H19 expression during the postnatal period. In contrast, silencing of c-Myc, a transcription factor that regulates H19 expression in other cell types (24; 25) and which is downregulated upon β -cell maturation had no effect on the level of this lncRNA (Supplementary Fig.3).

To elucidate the role of H19, we first investigated its function in the rat β -cell line INS832/13. Overexpression of H19 to reach levels comparable to those measured in neonatal islets (Supplementary Fig.4a), led to an increase in proliferation (Fig.2a) without effects on cell survival measured by scoring the pycnotic nuclei (Fig.2b) or by TUNEL assay (Supplementary Fig.5). The rise of H19 did also not affect insulin content or secretion (Fig.2c and d). Neonatal rat β -cells display a much higher proliferation rate compared to adult β -cells (10). To assess whether H19 contributes to postnatal β -cell expansion, the level of this lncRNA was reduced by RNA interference (Supplementary Fig.2b). Silencing of H19 in neonatal β -cells resulted in a profound decrease in proliferation both when assessed by scoring the number of Ki67⁺ (Fig.2e) and of

BrdU⁺ cells (Supplementary Fig.6). Moreover, restoration in adult rat islets of elevated levels of the lncRNA (Supplementary Fig.4c), induced a four-fold increase in the proliferating β -cells (Fig.2f). These effects were independent from Igf2 the levels of which were unchanged by the modulation of H19 expression (Supplementary Fig.7). Similar results were obtained upon overexpression of human H19 in the human β -cell line 1.1B4 (21) (Supplementary Fig.8).

H19 has been proposed to exert its action by affecting the level or the activity of different miRNAs (26-28). To investigate whether the regulation of β -cell proliferation is mediated by miRNAs, we assessed the effect of H19 in cells in which the expression of Argonaute 2 (Ago2), a component of the RNA-induced silencing complex (RISC) that is essential for miRNA action (29), is reduced by RNA interference (Supplementary Fig.2c). We observed that H19-induced proliferation is lost in INS832/13 cells lacking Ago2 (Fig.3a), indicating that H19 action may be mediated by miRNAs.

Two miRNAs, miR-675-5p and 3p, are produced upon processing of H19 (30). Indeed, overexpression of H19 in INS832/13 cells (Fig.3b and c) led to corresponding changes in the level of these miRNAs and silencing of H19 (Fig.3d and e), resulted in a decrease in miR-675-5p expression. Moreover, the expression profiles of these miRNAs throughout the postnatal period revealed a downregulation that parallels that of H19 (Fig.3f), suggesting that the effect of the lncRNA on β -cell proliferation may be mediated by these miRNAs. To assess this hypothesis, we transfected P5 islet cells with anti-miRs to block miR-675-5p or miR-675-3p (Supplementary Fig.9a and b). As shown in Fig.3g, while silencing of H19 reduced β -cell proliferation, blockade of miR-675-5p or miR-675-3p was without effect, indicating that the action of the lncRNA is likely to be independent from these miRNAs.

H19 expression is induced during myoblast differentiation and has been proposed to sequester the miRNA let-7 (31). The expression of most let-7 isoforms is not modified upon islet postnatal maturation (10), but possible changes in the repressive activity of these miRNAs have not yet been investigated. To evaluate the activity of let-7 in P10 and adult islets we transfected a reporter construct containing eight let-7 target sites in the 3' UTR of the *renilla* luciferase gene (32). We found that the luciferase activity of the let-7 sensor in adult rat islets is reduced compared to that of newborn islets, while the activity of a reporter lacking the let-7 target sites was not significantly different (Fig.4a), confirming a rise in the activity of let-7 family members

after postnatal maturation. Knock-down of let-7a with a specific inhibitor (Supplementary Fig.9c and d) led to an increase in proliferation of INS832/13 cells (Supplementary Fig.10). A similar tendency was observed in primary adult β -cells but the effect did not reach statistical significance, probably because of the presence of several other let-7 isoforms with overlapping functions. To circumvent this issue, adult β -cells were transfected with inhibitors targeting several let-7 family members (Supplementary Fig.9e). This resulted in a significant increase in β -cell proliferation (Fig.4b). In view of these findings, we hypothesized that H19 could induce β -cell proliferation by sequestering let-7, resulting in the de-repression of let-7 targets necessary for cell division. Using the RNAhybrid software (33), we identified several potential let-7 binding sites in the H19 sequence (Supplementary Fig.11) and generated a mutant lacking the two most likely let-7 target sequences (Supplementary Fig.12). To investigate if H19 acts by sequestering let-7, we overexpressed wild type and mutant H19 (Supplementary Fig.4b and d) and observed that the construct lacking the let-7 binding sites fails to trigger proliferation of INS832/13 and of dissociated adult islet cells (Fig.4c and d). These findings suggest that the proliferative effect of H19 may be at least in part mediated by preventing the interaction of let-7 with its endogenous target(s).

The PI3K-Akt signaling pathway is a critical regulator of the β -cell mass (34). We measured the activation of Akt after overexpression of wild type H19 or of its inactive mutant. We observed an increase in Akt phosphorylation after overexpression of wild type H19 but not upon overexpression of the inactive mutant (Fig.5a and b). Akt protein levels were unchanged (Supplementary Fig.13). Moreover, blockade of Akt phosphorylation using a pharmacological inhibitor (Fig.5c) prevented H19-induced proliferation of INS832/13 cells (Fig.5d) and of primary rat β -cells (Fig.5e). Similar results were obtained upon inhibition of PI3K activity with LY294002 (Supplementary Fig.14). Taken together, these findings indicate that H19 is likely to trigger β -cell proliferation by activating the PI3K-Akt signaling cascade.

In view of the role of H19 in the control of β -cell proliferation, we investigated whether the expression of this lncRNA is modified under conditions associated with changes in the β -cell mass. The administration of a low protein (LP) diet to rats during pregnancy has a major impact on the offspring, resulting in reduced birth weight, impaired β -cell development and a lower β -cell mass (18; 35). These features are associated with an increased risk of impaired glucose

tolerance and type 2 diabetes in adult life. We analyzed the expression of H19 and of E2F1 in the islets of 10 day-old pups born from mothers kept on control or LP diet. We found that the level of both transcripts is reduced in the islets of pups born from rat dams on an LP diet (Fig.6a and b), suggesting that altered levels of E2F1 and H19 may contribute to the decrease in β -cell mass in the LP offspring. The level of miR-675-5p and miR-675-3p tended also to be reduced but the decrease did not reach statistical significance (Fig.6c and d). The let-7a was in contrast slightly increased (Supplementary Fig.15), potentially contributing to a reduction in neonatal β -cell proliferation.

Ob/ob mice, which are leptin deficient, become severely obese but remain normoglycemic due to a compensatory expansion of their β -cell mass (36; 37). We found that the islets of ob/ob mice contain elevated levels of H19 compared to their wild-type littermates (Fig.7a). A similar increase in the expression of this lncRNA was also observed in the islets of insulin resistant and severely obese db/db mice lacking the leptin receptor and which become diabetic starting at about 6-8 weeks of age (Fig.7b). Note that an analogous trend of upregulation was found for E2F1 (data not shown) (38-40). To assess whether similar changes in H19 expression can be observed under conditions of acquired obesity, we measured the level of this lncRNA in the islets of mice fed with a high fat diet (HFD) during 8 weeks (19). The animals were classified in two groups according to their response to the diet, (i) low responders to HFD (LDR), with mild obesity, insulin resistance and normoglycemia, and (ii) high responders to HFD (HDR) with much higher obesity, insulin resistance and hyperglycemia, but also with a significant increase in β -cell proliferation and β -cell mass (19). We found H19 and E2F1 levels to be increased in the islets of the HDR group (Fig.7c and d). Moreover, we observed a positive correlation between weight gain and H19 levels (Fig.7e).

Together, our data suggest that in the face of insulin resistance re-expression of H19 may contribute to compensatory β -cell mass expansion in adulthood to achieve organismal glucose homeostasis.

DISCUSSION

Increasing evidence points to lncRNAs as integral components of the transcriptional machinery controlling pancreas development and β -cell function (15; 16; 41; 42). Although some lncRNAs have already been functionally linked to islet embryonic development (41) and to the regulation of adult β -cell activities (41), so far none of these transcripts has been formally linked to postnatal maturation of insulin-secreting cells, a critical process for the acquisition of adult β -cell function. A better understanding of the events underlying the maturation of β -cells is needed to unravel the developmental origins of diabetes predisposition and would be a leap forward for the engineering of functional insulin-secreting cells for the treatment of diabetes.

In this study, we detected 5496 lncRNAs expressed in newborn rat islets, 896 of which were upregulated and 1018 downregulated upon postnatal islet maturation. H19, a lncRNA conserved between rodents and humans, is one of the most strongly downregulated transcripts during the postnatal period in islet and FACS-sorted β -cells.

The *Igf2/H19* locus plays an important role in embryonic development and growth control (43). H19 is highly expressed during embryogenesis and is downregulated after birth in most tissues except in skeletal muscle and heart (44). We found that the transcription factor E2F1 is downregulated throughout β -cell maturation with kinetics superposing those of H19. E2F transcription factors play an important role in regulating cell survival and proliferation (45) and E2F1^{-/-} mice display impaired postnatal β -cell proliferation and maturation resulting in an overall reduction of pancreatic size and in glucose intolerance at the adulthood (45). Moreover, ectopic expression of E2F1 in adult β -cells increases the proliferation of insulin-secreting cells both in vitro and in vivo (46). We found that silencing of E2F1 causes a downregulation of H19 in immature islets, pointing to a prominent impact of this transcription factor on the control of H19 expression during the postnatal period.

Our data indicate that H19 is not involved in the regulation of insulin secretion but affect decisively β -cell proliferation. Indeed, silencing of this lncRNA reduces β -cell proliferation in newborn rats while restoration of elevated levels of H19 promotes proliferation of adult β -cells. This proliferative effect necessitates the activation of Akt and of PI3 kinase but the events triggering this signaling pathway remains to be fully elucidated. H19 has been proposed to

mediate its effects by modulating the activity of a group of miRNAs, either by sequestering them (31), by controlling miRNA maturation (47), or by directly generating two miRNAs, miR-675-5p and -3p, encoded in the first exon of the lncRNA (30). The hypothesis of an involvement of miRNAs in H19 action is corroborated by the loss of the proliferative capacity of H19 in the absence of Ago2, a core component of the RISC complex that is essential for miRNA function (29). These findings confirm a role for Ago2 in the induction of β -cell proliferation (48). In these experiments we did not observe a significant decrease in proliferation under control conditions, probably because a transient reduction of Ago2 may not be sufficient to impact on basal proliferation. The level of miR-675-5p and -3p is tightly linked to the expression of H19 during the entire postnatal period. However, blockade of miR-675-5p or of miR-675-3p does not affect proliferation of newborn β -cells, indicating that H19 is acting via a different mechanism. In skeletal muscle, H19 act by sequestering let-7 (31; 49). Several observations in this study suggest that a similar mechanism may operate in β -cells. Indeed, blockade of let-7 increases adult β -cell proliferation and removal of two let-7 binding sites in the sequence of H19 reduces the proliferative capacity of the lncRNA. Our data do not exclude the interaction of let-7 with other domains of H19 or the binding of other miRNAs. The repressive activity of let-7 is higher in adult rat islets, which contain much less H19 compared to newborn islets. Since the level of most let-7 family members is not modified upon β -cell maturation (10), these findings suggest that H19 may control the availability of let-7. A general schema summarizing the proposed role of H19 in the regulation of β -cell proliferation is shown in Fig.8. Our model does not preclude the existence additional mechanisms through which H19 can modulate β -cell proliferation. Indeed, H19 may regulate enhancer and promoter activities, resulting in changes in the expression of neighboring genes such as *Igf2*, *Cdkn1c*, *Kcnq1* and/or play important roles in the control of chromatin structure and of the imprinting regions.

Our data provide congruent grounds for the idea that H19 sustains β -cell expansion in newborns and is required to achieve an adequate postnatal β -cell mass. Thus, exposure to environmental conditions during gestation affecting the expression of H19 could potentially result in a β -cell mass insufficient to cover the organism needs. Indeed, we found that the level of H19 is reduced in the islets of offspring from dams on LP diet throughout gestation and lactation and that display an increased risk of impaired glucose tolerance and type 2 diabetes in adult life (35). Consistent with these observations, reduced H19 levels were previously observed in islets from offspring of

gestational diabetes mellitus (50), another adverse intrauterine condition linked to reduced β -cell proliferation and diabetes susceptibility at adulthood (51).

Adult β -cells undergo very little turnover and have low basal replication rates, which sustain metabolic homeostasis under normal conditions. However, pregnancy, obesity and β -cell recovery after injury are examples in which the systemic demand for insulin increases. To successfully compensate for the relative insulin deficiency that occurs during these metabolically pressured conditions, both proliferative and survival pathways are activated in insulin-secreting cells, to maintain blood glucose homeostasis and prevent the onset of diabetes (5). In this study, we observed the upregulation of H19 in different mouse models characterized by compensatory β -cell mass expansion in response to obesity and insulin resistance. These findings suggest that restoration of higher levels of H19 at adulthood in response to obesity associated insulin resistance may contribute to the expansion of the β -cell mass to counterbalance the diminished sensitivity of insulin target tissues and to prevent the onset of diabetes. Future studies involving the generation of gain and loss of function mice models will be needed to corroborate this hypothesis.

Taken together, our observations uncover an important role for H19 in the control of newborn and adult rodent β -cell proliferation and shed new light on the mechanisms potentially contributing to diabetes susceptibility in the offspring of dams on deleterious dietary conditions during pregnancy and lactation. The level of H19 was reported to be higher in β -cells of young children compared to those of adult donors, indicating that similar changes may occur in humans (52). Moreover, despite differences in the nucleotide sequence we obtained evidence that human H19 can exert proliferative effects similar to rat H19. However, the mechanisms driving rodent β -cell replication are often challenging to translate to humans. Thus, careful examination of the impact of H19 in primary human β -cells will be required before drawing definitive conclusions about the role of this non-coding RNA in humans.

Future efforts will be needed to fully capture the complexity of the events triggering compensatory β -cell expansion seen under physiological (pregnancy) and pathophysiological (obesity) conditions. This knowledge will contribute to the design of novel means to combat β -cell failure occurring in type 2 diabetes.

ACKNOWLEDGMENTS

The authors thank the IRCAN animal housing facility, genomics core and cytometry core (cytomed) and Dr. Y. Huang, Yale University, for providing the plasmid for the expression of human H19. This work was supported by grants from the Swiss National Science Foundation (310030-169480 (RR)), by the “Fondation Francophone pour la Recherche sur le Diabète” sponsored by the “Fédération Française des Diabétiques”, AstraZeneca, Eli Lilly, Merck Sharp & Dohme, Novo Nordisk and Sanofi (RR). EVO was supported by INSERM, Université Côte d’Azur, Conseil Régional PACA, Conseil Général des Alpes-Maritimes, Aviesan/AstraZeneca (Diabetes and the vessel wall injury program), the Agence Nationale de la Recherche (ANR) through ANR-RPV12004AAA (DIAMIR) “Investments for the Future” LABEX SIGNALIFE ANR-11-LABX-0028-01, and the European Foundation for the Study of Diabetes (EFSD/Lilly, European Diabetes Research Program). EVO team members are affiliated with the FHU OncoAge (<http://www.oncoage.org/>). MP is supported by grants from the Canadian Institutes of Health Research and holds the Canada Research Chair in Diabetes and Metabolism. DRL team is supported by a grant from the National Health and Medical Research Council of Australia.

DUALITY OF INTEREST

The authors declare that there is no duality of interest associated to this manuscript.

CONTRIBUTION STATEMENT

CS-P generated and analyzed the research data, wrote the manuscript and approved its final version. CJ, OD, KL, M-LP, CG, MP, DRL and EVO contributed to the acquisition or the analysis of the data, reviewed the manuscript and approved its final version. RR conceived the experiments, analyzed the research data, wrote the manuscript and approved its final version. RR is the guarantor of this work and, as such, had full access to all the data in the study and takes responsibility for the integrity of the data and the accuracy of the data analysis.

REFERENCES

1. Nolan CJ, Prentki M: The islet beta-cell: fuel responsive and vulnerable. *Trends Endocrinol Metab* 19:285-291, 2008
2. Freinkel N, Lewis NJ, Johnson R, Swenne I, Bone A, Hellerstrom C: Differential effects of age versus glycemic stimulation on the maturation of insulin stimulus-secretion coupling during culture of fetal rat islets. *Diabetes* 33:1028-1038, 1984
3. Hellerstrom C, Swenne I: Functional maturation and proliferation of fetal pancreatic beta-cells. *Diabetes* 40 Suppl 2:89-93, 1991
4. Wang P, Fiaschi-Taesch NM, Vasavada RC, Scott DK, Garcia-Ocana A, Stewart AF: Diabetes mellitus--advances and challenges in human beta-cell proliferation. *Nat Rev Endocrinol* 11:201-212, 2015
5. Liu Y MH, Ivanova A, Solimena M.: beta-Cells at the crossroads: choosing between insulin granule production and proliferation. *Diabetes Obes Metab* 10:1463-1326, 2009
6. Kapranov P, Cheng J, Dike S, Nix DA, Duttagupta R, Willingham AT, Stadler PF, Hertel J, Hackermuller J, Hofacker IL, Bell I, Cheung E, Drenkow J, Dumais E, Patel S, Helt G, Ganesh M, Ghosh S, Piccolboni A, Sementchenko V, Tammanna H, Gingeras TR: RNA maps reveal new RNA classes and a possible function for pervasive transcription. *Science* 316:1484-1488, 2007
7. Mercer TR, Dinger ME, Mattick JS: Long non-coding RNAs: insights into functions. *Nat Rev Genet* 10:155-159, 2009
8. Ponting CP, Oliver PL, Reik W: Evolution and functions of long noncoding RNAs. *Cell* 136:629-641, 2009
9. Wilusz JE, Sunwoo H, Spector DL: Long noncoding RNAs: functional surprises from the RNA world. *Genes Dev* 23:1494-1504, 2009
10. Jacovetti C, Matkovich SJ, Rodriguez-Trejo A, Guay C, Regazzi R: Postnatal beta-cell maturation is associated with islet-specific microRNA changes induced by nutrient shifts at weaning. *Nat Commun* 6:8084, 2015
11. Rinn JL, Chang HY: Genome regulation by long noncoding RNAs. *Annu Rev Biochem* 81:145-166, 2012
12. Derrien T, Johnson R, Bussotti G, Tanzer A, Djebali S, Tilgner H, Guernec G, Martin D, Merkel A, Knowles DG, Lagarde J, Veeravalli L, Ruan X, Ruan Y, Lassmann T, Carninci P, Brown JB, Lipovich L, Gonzalez JM, Thomas M, Davis CA, Shiekhattar R, Gingeras TR, Hubbard TJ, Notredame C, Harrow J, Guigo R: The GENCODE v7 catalog of human long noncoding RNAs: analysis of their gene structure, evolution, and expression. *Genome Res* 22:1775-1789, 2012
13. Batista PJ, Chang HY: Long noncoding RNAs: cellular address codes in development and disease. *Cell* 152:1298-1307, 2013
14. Ku GM, Kim H, Vaughn IW, Hangauer MJ, Myung Oh C, German MS, McManus MT: Research resource: RNA-Seq reveals unique features of the pancreatic beta-cell transcriptome. *Mol Endocrinol* 26:1783-1792, 2012
15. Moran I, Akerman I, van de Bunt M, Xie R, Benazra M, Nammo T, Arnes L, Nakic N, Garcia-Hurtado J, Rodriguez-Segui S, Pasquali L, Sauty-Colace C, Beucher A, Scharfmann R, van Arensbergen J, Johnson PR, Berry A, Lee C, Harkins T, Gmyr V, Pattou F, Kerr-Conte J, Piemonti L, Berney T, Hanley N, Gloyn AL, Sussel L, Langman L, Brayman KL, Sander M, McCarthy MI, Ravassard P, Ferrer J: Human beta cell transcriptome analysis uncovers lncRNAs that are tissue-specific, dynamically regulated, and abnormally expressed in type 2 diabetes. *Cell Metab* 16:435-448, 2012
16. Motterle A, Gattesco S, Peyot ML, Esguerra JLS, Gomez-Ruiz A, Laybutt DR, Gilon P, Burdet F, Ibberson M, Eliasson L, Prentki M, Regazzi R: Identification of islet-enriched long non-coding RNAs contributing to beta-cell failure in type 2 diabetes. *Mol Metab* 6:1407-1418, 2017
17. Zemel S, Bartolomei MS, Tilghman SM: Physical linkage of two mammalian imprinted genes, H19 and insulin-like growth factor 2. *Nat Genet* 2:61-65, 1992

18. Dumortier O, Hinault C, Gautier N, Patouraux S, Casamento V, Van Obberghen E: Maternal protein restriction leads to pancreatic failure in offspring: role of misexpressed microRNA-375. *Diabetes* 63:3416-3427, 2014
19. Peyot ML, Pepin E, Lamontagne J, Latour MG, Zarrouki B, Lussier R, Pineda M, Jetton TL, Madiraju SR, Joly E, Prentki M: Beta-cell failure in diet-induced obese mice stratified according to body weight gain: secretory dysfunction and altered islet lipid metabolism without steatosis or reduced beta-cell mass. *Diabetes* 59:2178-2187, 2010
20. Hohmeier HE, Mulder H, Chen G, Henkel-Rieger R, Prentki M, Newgard CB: Isolation of INS-1-derived cell lines with robust ATP-sensitive K⁺ channel-dependent and -independent glucose-stimulated insulin secretion. *Diabetes* 49:424-430, 2000
21. McCluskey JT, Hamid M, Guo-Parke H, McClenaghan NH, Gomis R, Flatt PR: Development and functional characterization of insulin-releasing human pancreatic beta cell lines produced by electrofusion. *J Biol Chem* 286:21982-21992, 2011
22. Gotoh M, Maki T, Satomi S, Porter J, Bonner-Weir S, O'Hara CJ, Monaco AP: Reproducible high yield of rat islets by stationary in vitro digestion following pancreatic ductal or portal venous collagenase injection. *Transplantation* 43:725-730, 1987
23. Kohler M, Dare E, Ali MY, Rajasekaran SS, Moede T, Leibiger B, Leibiger IB, Tibell A, Juntti-Berggren L, Berggren PO: One-step purification of functional human and rat pancreatic alpha cells. *Integr Biol (Camb)* 4:209-219, 2012
24. Cui J, Mo J, Luo M, Yu Q, Zhou S, Li T, Zhang Y, Luo W: c-Myc-activated long non-coding RNA H19 downregulates miR-107 and promotes cell cycle progression of non-small cell lung cancer. *Int J Clin Exp Pathol* 8:12400-12409, 2015
25. Zhang EB, Han L, Yin DD, Kong R, De W, Chen J: c-Myc-induced, long, noncoding H19 affects cell proliferation and predicts a poor prognosis in patients with gastric cancer. *Med Oncol* 31:914, 2014
26. Liang WC, Fu WM, Wang YB, Sun YX, Xu LL, Wong CW, Chan KM, Li G, Waye MM, Zhang JF: H19 activates Wnt signaling and promotes osteoblast differentiation by functioning as a competing endogenous RNA. *Sci Rep* 6:20121, 2016
27. Liang WC, Fu WM, Wong CW, Wang Y, Wang WM, Hu GX, Zhang L, Xiao LJ, Wan DC, Zhang JF, Waye MM: The lncRNA H19 promotes epithelial to mesenchymal transition by functioning as miRNA sponges in colorectal cancer. *Oncotarget* 6:22513-22525, 2015
28. Liu L, Yang J, Zhu X, Li D, Lv Z, Zhang X: Long noncoding RNA H19 competitively binds miR-17-5p to regulate YES1 expression in thyroid cancer. *FEBS J* 283:2326-2339, 2016
29. Guo H, Ingolia NT, Weissman JS, Bartel DP: Mammalian microRNAs predominantly act to decrease target mRNA levels. *Nature* 466:835-840, 2010
30. Cai X, Cullen BR: The imprinted H19 noncoding RNA is a primary microRNA precursor. *RNA* 13:313-316, 2007
31. Kallen AN, Zhou XB, Xu J, Qiao C, Ma J, Yan L, Lu L, Liu C, Yi JS, Zhang H, Min W, Bennett AM, Gregory RI, Ding Y, Huang Y: The imprinted H19 lncRNA antagonizes let-7 microRNAs. *Mol Cell* 52:101-112, 2013
32. Iwasaki S, Kawamata T, Tomari Y: Drosophila argonaute1 and argonaute2 employ distinct mechanisms for translational repression. *Mol Cell* 34:58-67, 2009
33. Rehmsmeier M, Steffen P, Hochsmann M, Giegerich R: Fast and effective prediction of microRNA/target duplexes. *RNA* 10:1507-1517, 2004
34. Fatrai S, Elghazi L, Balcazar N, Cras-Meneuve C, Krits I, Kiyokawa H, Bernal-Mizrachi E: Akt induces beta-cell proliferation by regulating cyclin D1, cyclin D2, and p21 levels and cyclin-dependent kinase-4 activity. *Diabetes* 55:318-325, 2006
35. Cox AR, Gotthel SK, Arany EJ, Hill DJ: The effects of low protein during gestation on mouse pancreatic development and beta cell regeneration. *Pediatr Res* 68:16-22, 2010
36. Lindstrom P: The physiology of obese-hyperglycemic mice [ob/ob mice]. *ScientificWorldJournal* 7:666-685, 2007

37. Chan JY, Luzuriaga J, Bensellam M, Biden TJ, Laybutt DR: Failure of the adaptive unfolded protein response in islets of obese mice is linked with abnormalities in beta-cell gene expression and progression to diabetes. *Diabetes* 62:1557-1568, 2013
38. Chen H, Charlat O, Tartaglia LA, Woolf EA, Weng X, Ellis SJ, Lakey ND, Culpepper J, Moore KJ, Breitbart RE, Duyk GM, Tepper RI, Morgenstern JP: Evidence that the diabetes gene encodes the leptin receptor: identification of a mutation in the leptin receptor gene in db/db mice. *Cell* 84:491-495, 1996
39. Kjørholt C, Akerfeldt MC, Biden TJ, Laybutt DR: Chronic hyperglycemia, independent of plasma lipid levels, is sufficient for the loss of beta-cell differentiation and secretory function in the db/db mouse model of diabetes. *Diabetes* 54:2755-2763, 2005
40. Dalbøge LS, Almholt DL, Neerup TS, Vassiliadis E, Vrang N, Pedersen L, Fosgerau K, Jelsing J: Characterisation of age-dependent beta cell dynamics in the male db/db mice. *PLoS One* 8:e82813, 2013
41. Arnes L, Akerman I, Balderes DA, Ferrer J, Sussel L: betalincl encodes a long noncoding RNA that regulates islet beta-cell formation and function. *Genes Dev* 30:502-507, 2016
42. Motterle A, Gattesco S, Caille D, Meda P, Regazzi R: Involvement of long non-coding RNAs in beta cell failure at the onset of type 1 diabetes in NOD mice. *Diabetologia* 58:1827-1835, 2015
43. Gabory A, Ripoché MA, Le Digarcher A, Watrin F, Ziyyat A, Forne T, Jammes H, Ainscough JF, Surani MA, Journot L, Dandolo L: H19 acts as a trans regulator of the imprinted gene network controlling growth in mice. *Development* 136:3413-3421, 2009
44. Poirier F, Chan CT, Timmons PM, Robertson EJ, Evans MJ, Rigby PW: The murine H19 gene is activated during embryonic stem cell differentiation in vitro and at the time of implantation in the developing embryo. *Development* 113:1105-1114, 1991
45. Fajas L, Annicotte JS, Miard S, Sarruf D, Watanabe M, Auwerx J: Impaired pancreatic growth, beta cell mass, and beta cell function in E2F1 (-/-) mice. *J Clin Invest* 113:1288-1295, 2004
46. Grouwels G, Cai Y, Hoebeke I, Leuckx G, Heremans Y, Ziebold U, Stange G, Chintinne M, Ling Z, Pipeleers D, Heimberg H, Van de Casteele M: Ectopic expression of E2F1 stimulates beta-cell proliferation and function. *Diabetes* 59:1435-1444, 2010
47. Giovarelli M, Bucci G, Ramos A, Bordo D, Wilusz CJ, Chen CY, Puppo M, Briata P, Gherzi R: H19 long noncoding RNA controls the mRNA decay promoting function of KSRP. *Proc Natl Acad Sci U S A* 111:E5023-5028, 2014
48. Tattikota SG, Rathjen T, McAnulty SJ, Wessels HH, Akerman I, van de Bunt M, Hausser J, Esguerra JL, Musahl A, Pandey AK, You X, Chen W, Herrera PL, Johnson PR, O'Carroll D, Eliasson L, Zavolan M, Gloyne AL, Ferrer J, Shalom-Feuerstein R, Aberdam D, Poy MN: Argonaute2 mediates compensatory expansion of the pancreatic beta cell. *Cell Metab* 19:122-134, 2014
49. Gao Y, Wu F, Zhou J, Yan L, Jurczak MJ, Lee HY, Yang L, Mueller M, Zhou XB, Dandolo L, Szendroedi J, Roden M, Flannery C, Taylor H, Carmichael GG, Shulman GI, Huang Y: The H19/let-7 double-negative feedback loop contributes to glucose metabolism in muscle cells. *Nucleic Acids Res* 42:13799-13811, 2014
50. Ding GL, Wang FF, Shu J, Tian S, Jiang Y, Zhang D, Wang N, Luo Q, Zhang Y, Jin F, Leung PC, Sheng JZ, Huang HF: Transgenerational glucose intolerance with Igf2/H19 epigenetic alterations in mouse islet induced by intrauterine hyperglycemia. *Diabetes* 61:1133-1142, 2012
51. Kahraman S, Dirice E, De Jesus DF, Hu J, Kulkarni RN: Maternal insulin resistance and transient hyperglycemia impact the metabolic and endocrine phenotypes of offspring. *Am J Physiol Endocrinol Metab* 307:E906-918, 2014
52. Arda HE, Li L, Tsai J, Torre EA, Rosli Y, Peiris H, Spitale RC, Dai C, Gu X, Qu K, Wang P, Wang J, Grompe M, Scharfmann R, Snyder MS, Bottino R, Powers AC, Chang HY, Kim SK: Age-Dependent Pancreatic Gene Regulation Reveals Mechanisms Governing Human beta Cell Function. *Cell Metab* 23:909-920, 2016

FIGURE LEGENDS

Fig.1) Comparison of lncRNA expression between 10-day old and adult rat islets and regulation of H19 expression. (a) Volcano Plot representing the lncRNAs differentially expressed between P10 and adult islets. Up- or downregulated transcripts are depicted in red (nominal $P < 0.05$, Fold change $\geq |2|$). H19 is indicated by the arrow. (b) Selected lncRNA with p-value, fold change, regulation and type. The expression of H19 and E2F1 was measured by qRT-PCR in P10 and adult islets (c) or FACS-sorting purified β -cells (d). (e) Expression of H19 and E2F1 in islets at the indicated ages was determined by qRT-PCR, normalized to 18S and expressed in fold change vs. P1. (f) Dissociated P10 rat islet cells were transfected with a siRNA against GFP or E2F1 for 48h. The expression of H19 was measured by qRT-PCR and expressed as fold change compared to control. The results are means \pm SEM of three (d) or four (c,e,f) independent experiments per group. * $p < 0.05$, ** $p < 0.01$, *** $P < 0.001$, **** $P < 0.0001$ were determined by Student's t-test or by one-way ANOVA with a Dunnett post-hoc test when more than 2 sets of data were analyzed.

Fig.2) Functional role of H19 in β -cells. INS832/13 cells (a,b,c,d) or dissociated adult rat islet cells (f) were transfected with a control plasmid (pcDNA3) or a plasmid allowing the expression of H19 for 48h. (a,f) The fraction of proliferating cells was determined by scoring Ki67 positive cells. (b) Cell death was assessed by scoring the cells displaying pycnotic nuclei. The cells were incubated for the last 24h without or with a mix of cytokines. (c) Insulin secretion and insulin content (d) were measured by ELISA after 45 min of incubation with either 2mM or 20mM of glucose. (e) Dissociated P10 rat islet cells were transfected with a siRNA against GFP or H19. The fraction of proliferating insulin-expressing cells was determined by scoring Ki67 positive cells. The results are the means \pm SEM of three (b,e), four (f) five (c,d) or seven (a) independent experiments. Statistical differences from control conditions were assessed by Student's t-test or by one-way ANOVA with a Dunnett post-hoc test when more than two conditions were compared. * $P < 0.05$.

Fig.3) Involvement of miRNAs in H19 action. (a) INS832/13 cells were co-transfected with a siRNA against GFP or Ago2 (siGFP or siAgo2) and a control plasmid (pcDNA3) or a plasmid overexpressing H19. 48 h later, the fraction of proliferating cells was determined by scoring Ki67

positive cells. **(b,c)** INS832/13 cells were transfected for 48 h with a control plasmid (pcDNA3) or a plasmid expressing H19. **(d,e)** Dissociated P5 rat islet cells were transfected for 48 h with a siRNA against GFP or H19. miR-675-5p and -3p levels were measured by qRT-PCR, normalized to those of miR-130b-3p and expressed in fold change vs control condition (first column for each graph) or P1 levels for the postnatal islet time course expression **(f)**. **(g)** Dissociated P5 rat islet cells were transfected with a control, a miR-675-5p or -3p inhibitor or with a siRNA against GFP or H19. 48 h later, the fraction of proliferating insulin-expressing cells was assessed by scoring Ki67 positive cells. The results are means \pm SEM of three **(a-e)** or five **(f)** independent experiments. Statistical differences from control conditions were determined by Student's t-test or by one-way ANOVA with a Dunnett **(a,f)** or Tukey **(g)** post-hoc test, when more than 2 sets of data were analyzed. * $p < 0.05$, *** $P < 0.001$, **** $P < 0.0001$.

Fig.4) Let-7 family members participate in H19 action in β -cells. **(a)** Dissociated P10 or adult islet cells were transfected with a luciferase constructs containing (blue dots) or lacking (red dots) eight target sites for let-7 in its 3' UTR. Luciferase activity was measured 48 h later. **(b)** Dissociated adult rat islet cells were transfected with a control inhibitor or with anti-miRs blocking all let-7 family members. INS832/13 cells **(c)** and dissociated adult rat islet cells **(d)** were transfected with a control plasmid (pcDNA3), a plasmid overexpressing H19 or a plasmid overexpressing a H19 form without let-7 binding sites (H19 Δ). Two days later, the fraction of proliferating insulin-expressing cells was assessed by scoring Ki67 positive cells. The results correspond to the means \pm SEM of three **(a,b,c)** or four **(d)** independent experiments. Statistical differences from control conditions were calculated by Student's t-test or by one-way ANOVA with a Dunnett post-hoc test when more than two sets of data were analyzed. * $p < 0.05$.

Fig.5) H19 induces β -cell proliferation via the activation of Akt. **(a)** Representative western blot analysis of Akt phosphorylation at Thr-308 (P-Akt) in INS832/13 cells transfected with a control plasmid (pcDNA3), a plasmid overexpressing H19 or a H19 form without two binding sites for let-7 (H19 Δ). **(b)** The Western blots were analyzed by densitometry scanning and the abundance of P-Akt bands was normalized to that of actin α . **(c,d)** INS832/13 cells or primary rat islet cells **(e)** were transfected with a control plasmid (pcDNA3) or a plasmid expressing H19. After 48h, cells were exposed or not for 2h to 10 μ M of the Akt inhibitor (Anti-Akt; ab142088). **(c)** Representative western blot analysis of AKT phosphorylation at Ser-478 (P-Akt) and Akt

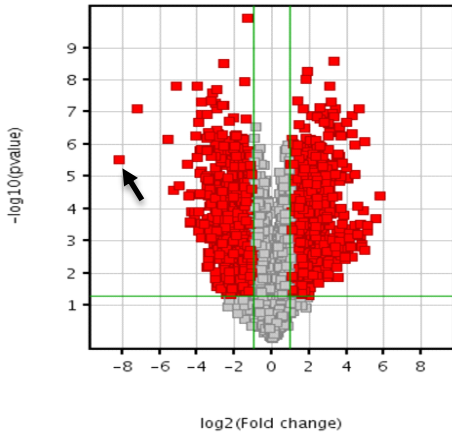
protein expression. **(d,e)** The fraction of proliferating insulin-expressing cells was assessed by scoring those that were positive for Ki67. The results are means±SEM of three **(d,e)** or four **(b)** independent experiments. Statistical differences from control conditions were assessed by Kruskal-Wallis test with a Dunn post-hoc test **(b)** or by one-way ANOVA with a Dunnett post-hoc test **(d,e)**. *P<0.05.

Fig.6) Expression of H19, E2F1, miR-675-5p and miR-675-3p in islets of offspring from low-protein diet gestation and lactation. H19 **(a)**, E2F1 **(b)**, miR-675-5p **(c)** and miR-675-3p **(d)** islet levels were measured by qRT-PCR in P10 control rats (Control) and P10 rat offspring from low-protein diet during gestation (LP), normalized to those of Ppia **(a,b)** or miR-130b-3p **(c,d)** and expressed in fold change. The results correspond to the means±SEM of four or six different individuals. Statistical differences from control pups were calculated by Student's t-test: *p<0.05.

Fig.7) H19 participates in β-cell mass expansion under obesity associated insulin resistance conditions. RNA levels were measured by qRT-PCR in islets from wt/wt and ob/ob mice **(a)**, from wt/db and db/db mice **(b)**, and in islets of mice fed with a normal chow diet (ND) or with high fat diet: low diet responders (LDR) and high diet responders (HFD) **(c,d)**. **(e)** Linear regression analysis between H19 levels and weight before sacrifice of mice fed with a normal or high fat diet. Statistical differences from control mice (wt/wt, wt/db or ND) were calculated by Student's t-test **(a,b)**, by Kruskal-Wallis test with a Dunn post-hoc test **(c)** or by one-way ANOVA with a Dunnett post-hoc test **(d)**. F-test was performed to measure significance in **e**. *P<0.05.

Fig.8) Model representing our view on the role of H19 in the control of β-cell proliferation. We propose a positive feedback loop, where growth stimuli activate the PI3K and trigger the phosphorylation of Akt. This induces the activation of cyclin/cdk complexes that phosphorylate Rb, causing the release and the activation of E2F1. This results in a rise in H19 expression that binds let-7, relieving the repression of the targets of these miRNAs and further enhancing the activation of the PI3K/Akt pathway and cell cycle entry. Solid arrows indicate proven interactions while dotted lines show putative mechanisms inferred from our observations.

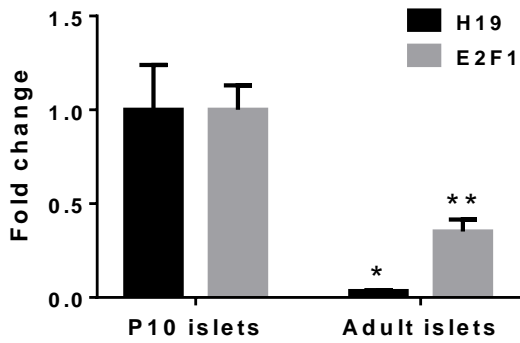
a



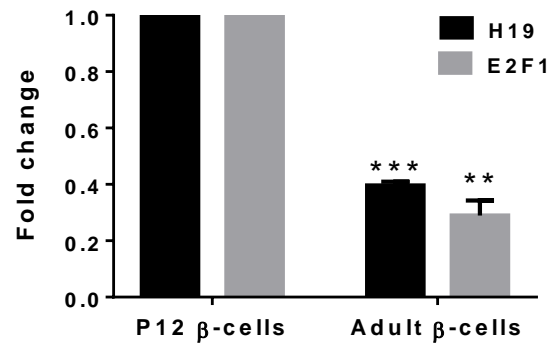
b

Adult versus newborn rat islets				
ID	P-value	Fold change	Regulation	Type
NR_027324 (H19)	3^E-06	303	Down	Intergenic

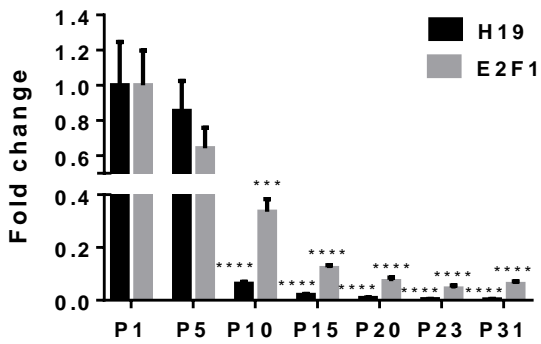
c



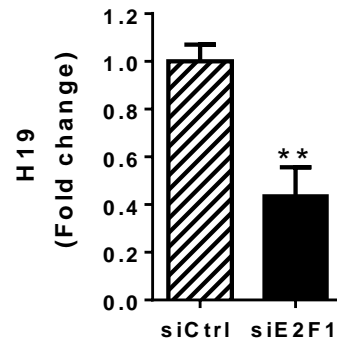
d

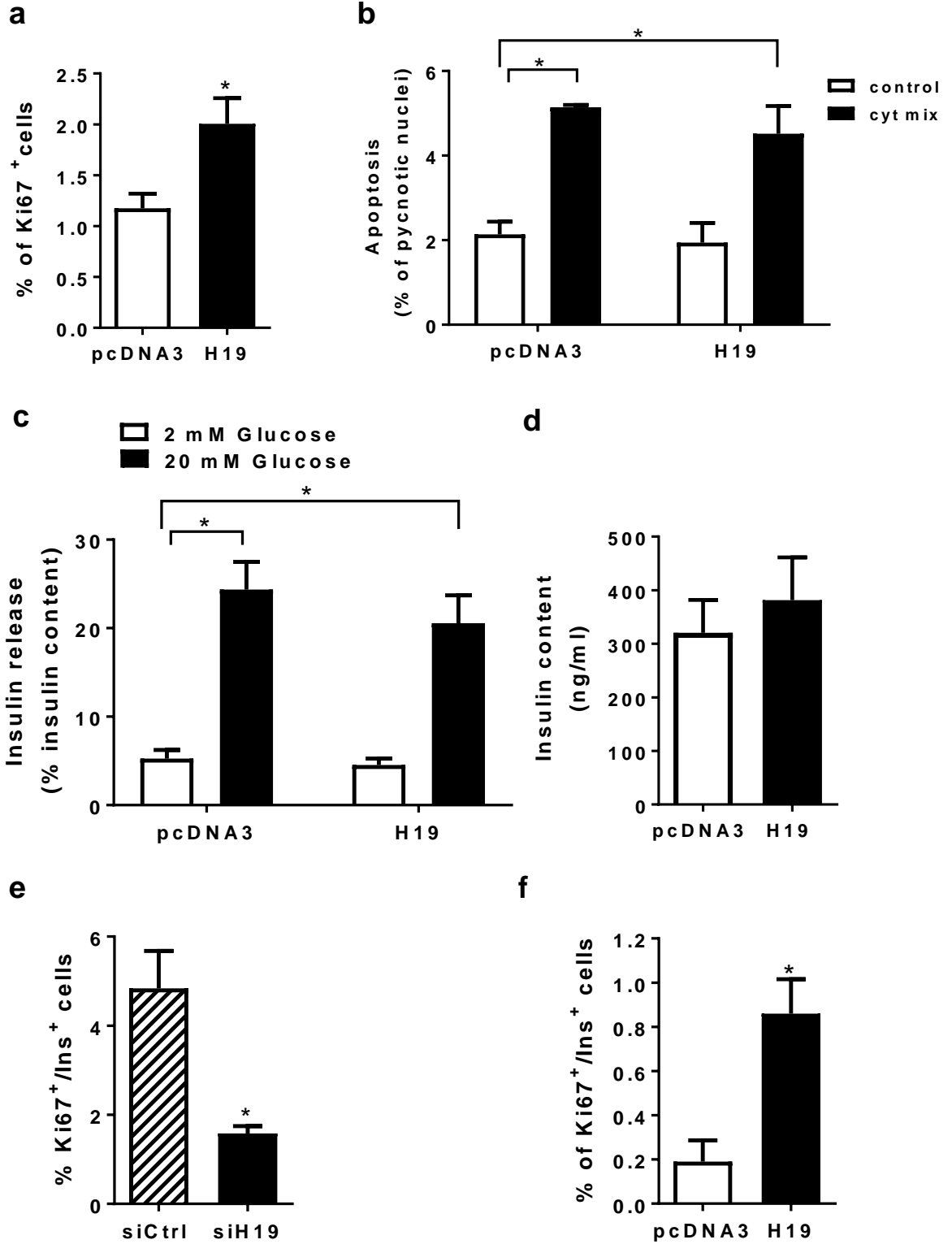


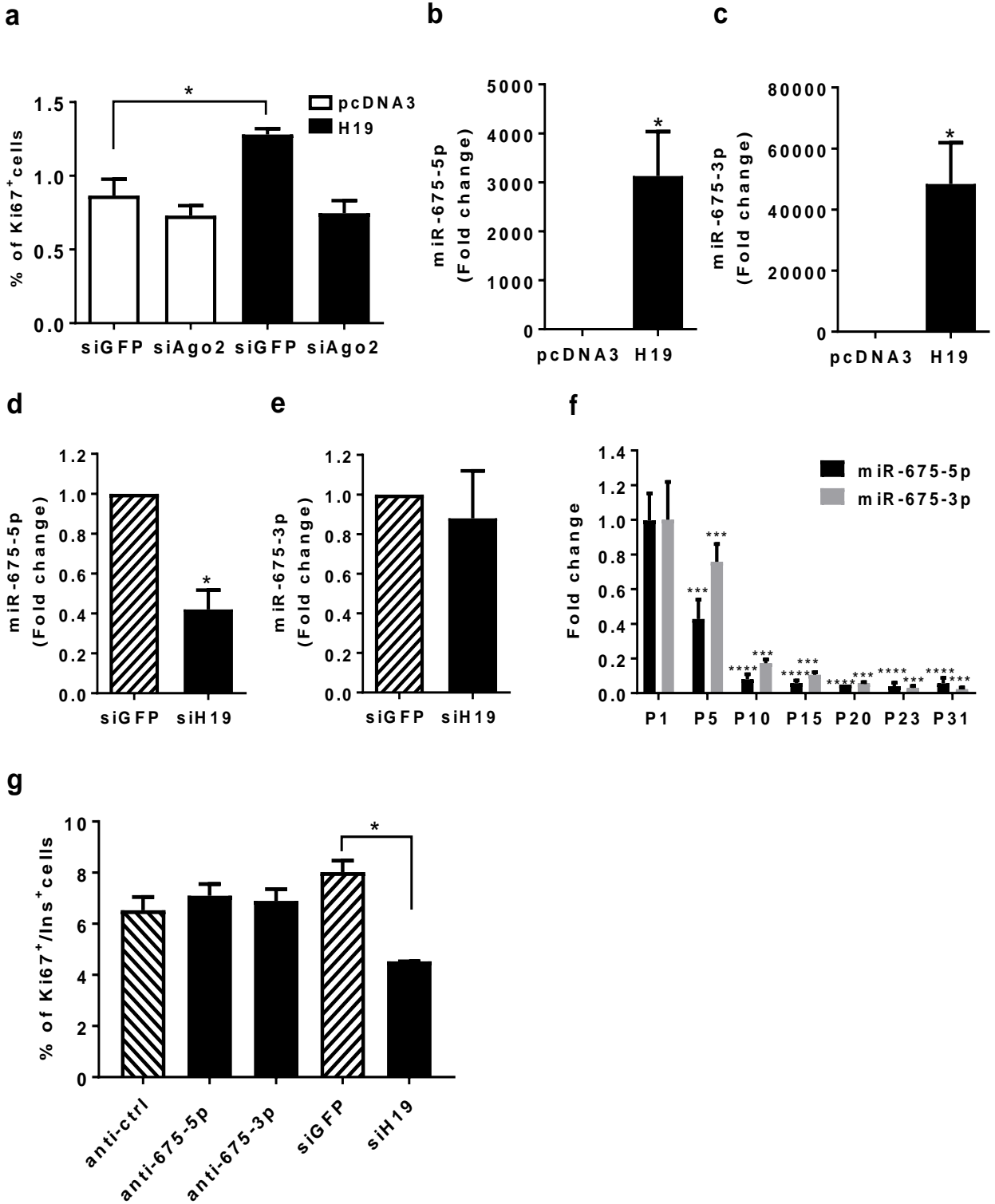
e

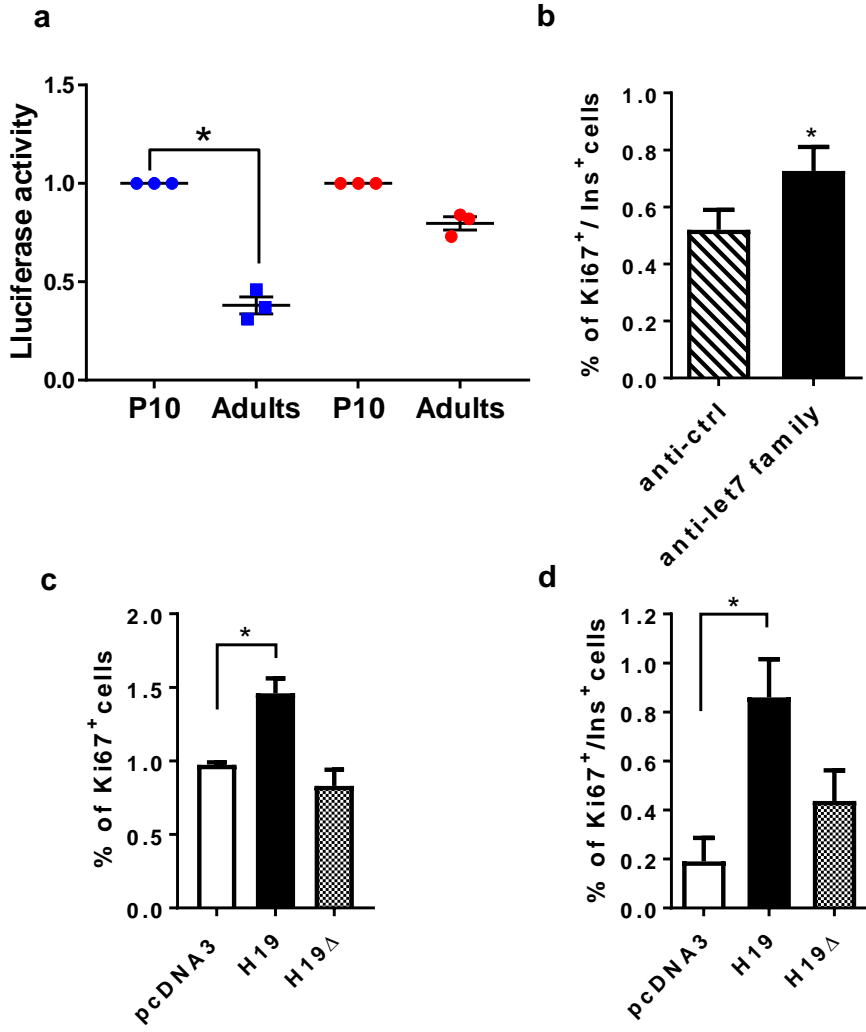


f

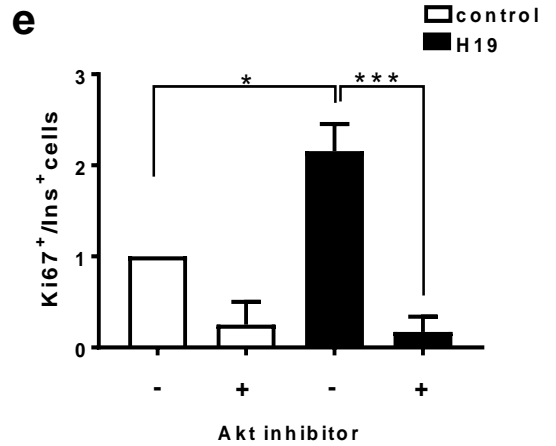
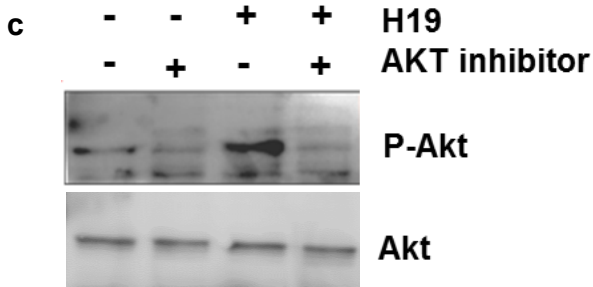
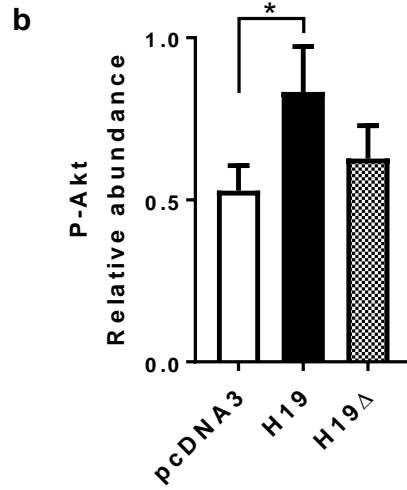
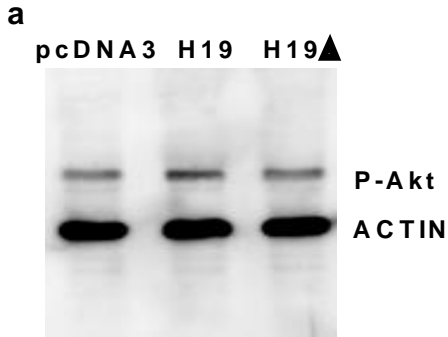




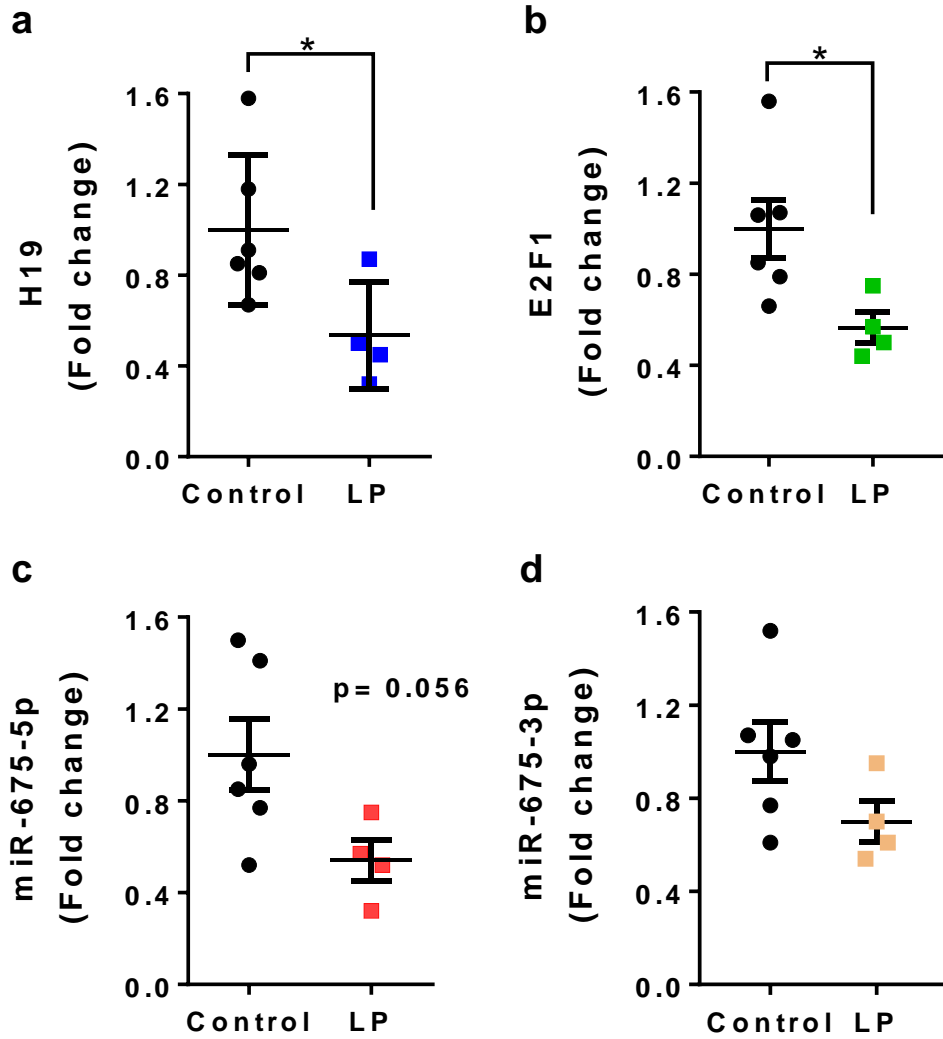


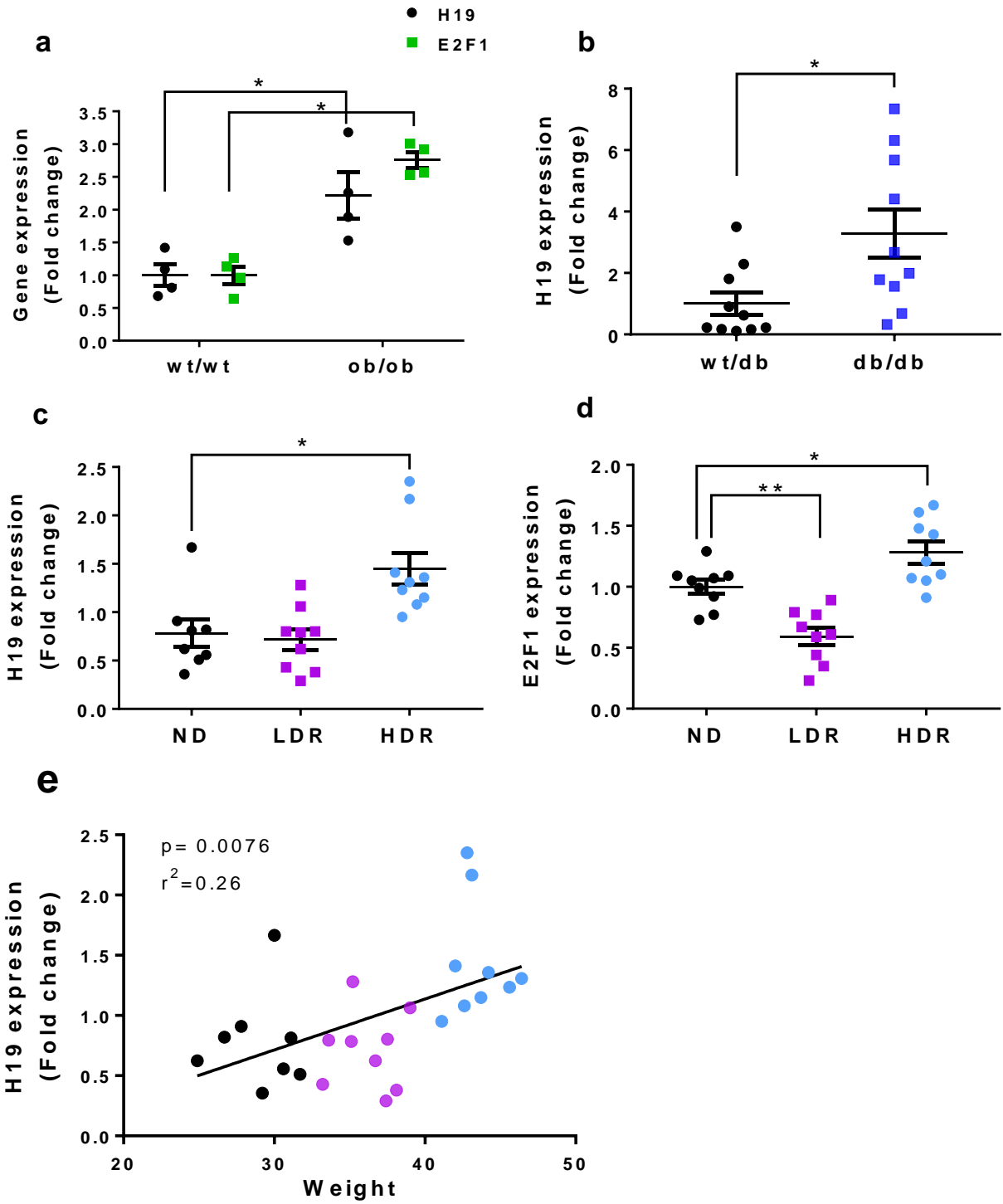


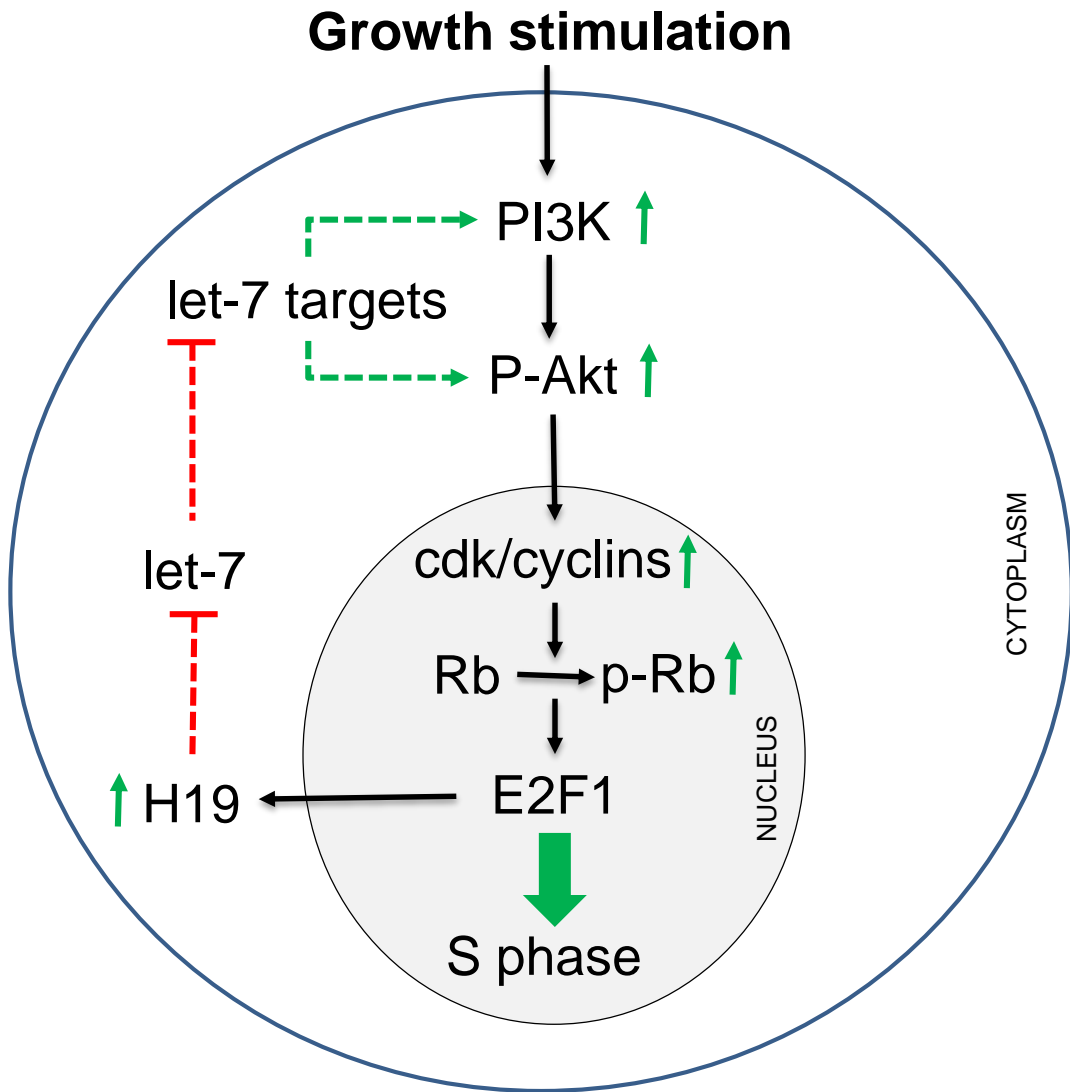
Sanchez_Fig5



Sanchez_Fig6



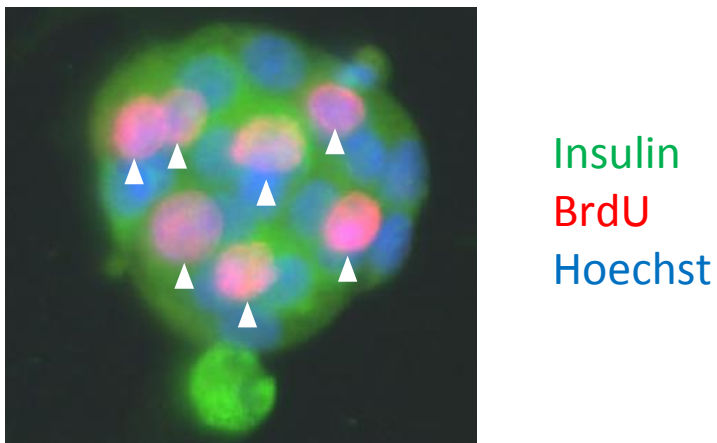
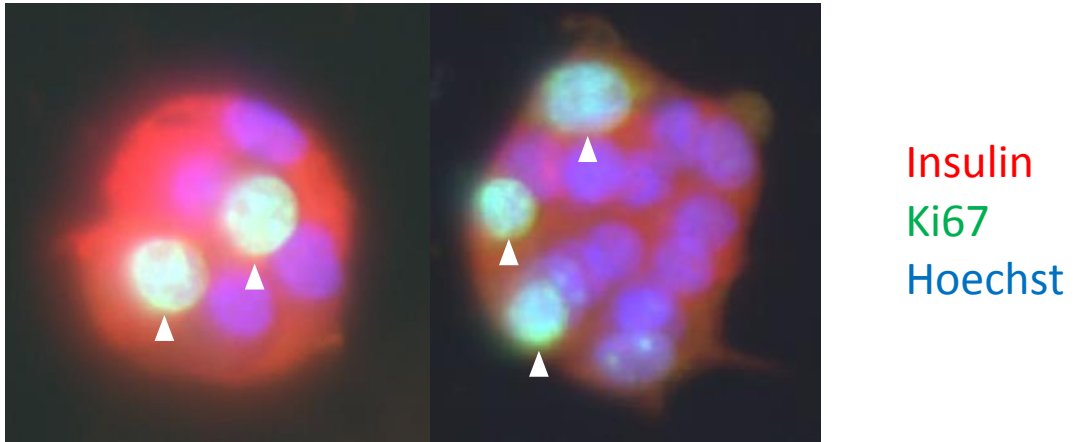




Supplementary table 1. List of primers used for measuring RNA levels by qRT-PCR.

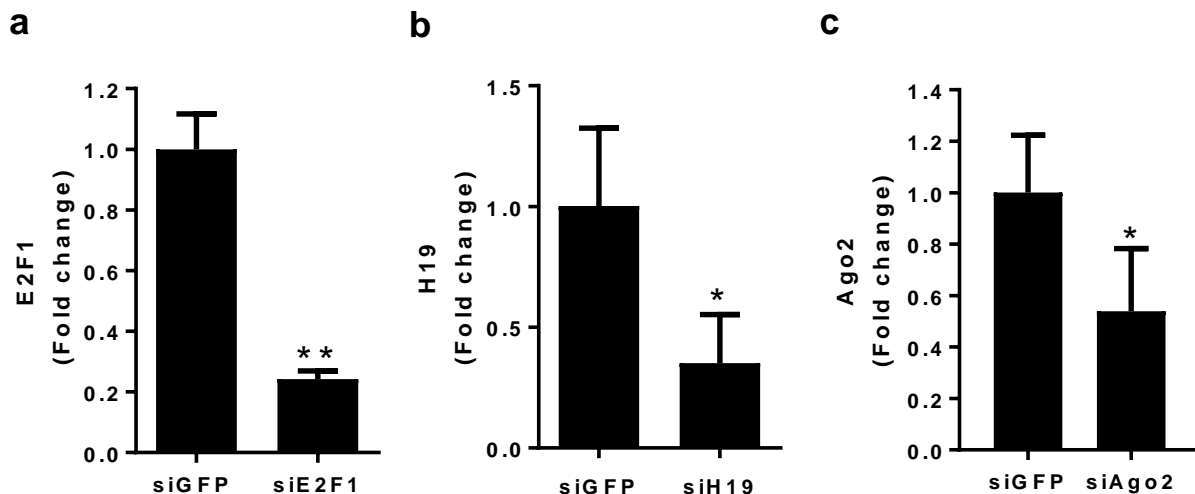
Specie	Primer name	Sequence
Rat	<i>Ago2-F</i>	5'-CCAGATGAAGAACGTGCAGA-3'
	<i>Ago2-R</i>	5'-CGGCAGCAATTGAAGGTTTC-3'
Rat	<i>c-Myc-F</i>	5'-CGAGCTGAAGCGTAGCTTTT-3'
	<i>c-Myc-R</i>	5'-CTCGCCGTTTCCTCAGTAAG-3'
Rat	<i>E2f1-F</i>	5'-GGCAAACCTGGGGAATAAGC-3'
	<i>E2f1-R</i>	5'-ATGGCTGTCAGTCTGTCTCC-3'
Mouse	<i>E2f1-F</i>	5'-CCCTACCCAAGAGTTGCTGA-3'
	<i>E2f1-R</i>	5'-TAGGAAGGACGCATACCCAC-3'
Rat	<i>Gapdh-F</i>	5'-ATGGTGAAGGTCGGTGTGAA-3'
	<i>Gapdh-R</i>	5'-TCTCGCTCCTGGAAGATGG-3'
Mouse	<i>Gapdh-F</i>	5'-TGCACCACCAACTGCTTAGC-3'
	<i>Gapdh-R</i>	5'-GGCATGGACTGTGGTCATGAG-3'
Rat and mouse	<i>Hprt1-F</i>	5'-AGTCCCAGCGTCGTGATTAG-3'
	<i>Hprt1-R</i>	5'-AATCCAGCAGGTCAGCAAAG-3'
Human	<i>Hprt1-F</i>	5'-CCCTGGCGTCGTGATTAGTG-3'
	<i>Hprt1-R</i>	5'-GCTACAATGTGATGGCCTCCC-3'
Rat	<i>H19-F</i>	5'-GCCTGAGTCTCTCCGTATGG-3'
	<i>H19-R</i>	5'-GAAGGAAGGTGCGTTGAACA-3'
Mouse	<i>H19-F</i>	5'-AATGGTGCTACCCAGCTCAT-3'
	<i>H19-R</i>	5'-TCAGAACGAGACGGACTTAAAGAA-3'
Human	<i>H19-F</i>	5'-GCACCTTGGACATCTGGAGT-3'
	<i>H19-R</i>	5'-TTCTTTCCAGCCCTAGCTCA-3'
Rat	<i>Igf2-F</i>	5'-GGGACGTGTCTACCTCTCAG-3'
	<i>Igf2-R</i>	5'-GTAACACGATCAGGGGACGG-3'
Rat	<i>Ppia-F</i>	5'-CCACCGTGTTCTTCGACATC-3'
	<i>Ppia-R</i>	5'-TTGCCACCAGTGCCATTATG-3'
Rat	<i>18s-F</i>	5'-GCAAATTACCCACTCCCGAC-3'
	<i>18s-R</i>	5'-CCGCTCCCAAGATCCAATA-3'

Supplementary figure 1



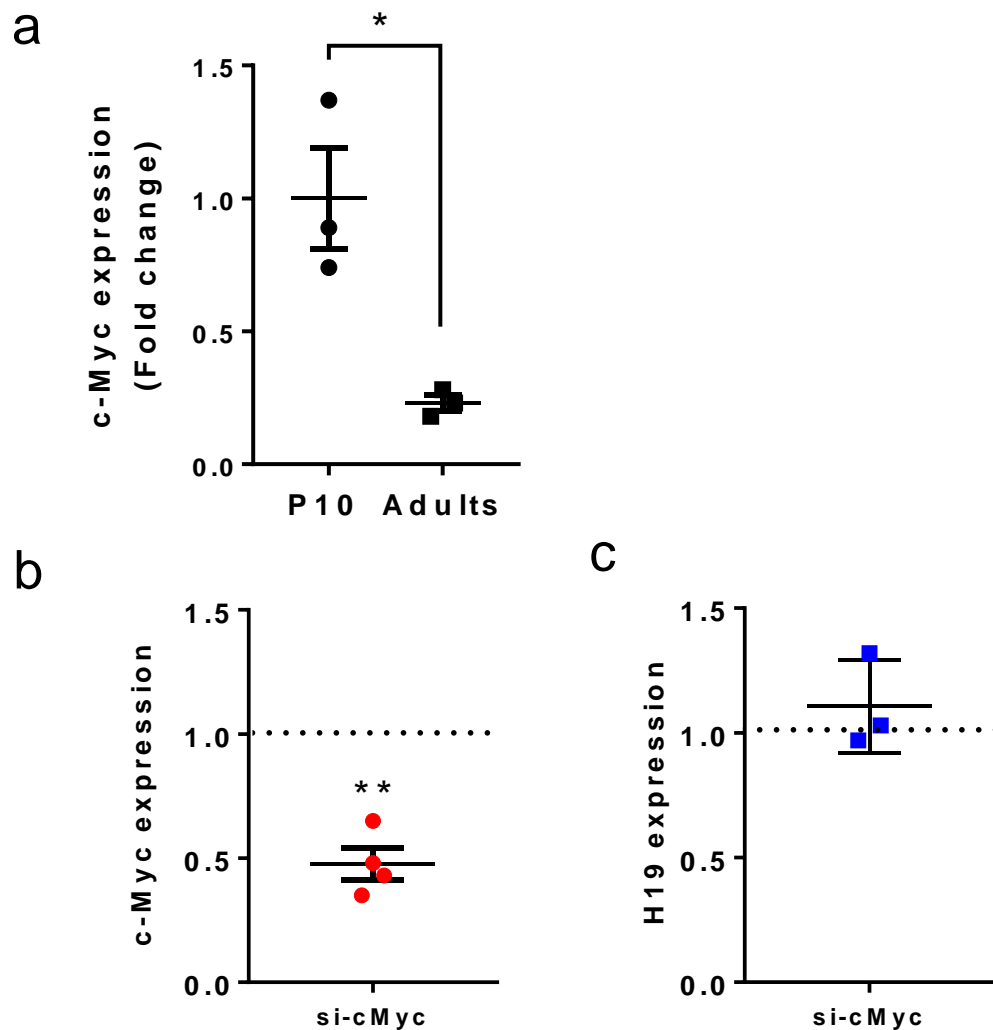
Supplementary Fig.1. Representative images of primary rat β -cells double positive for insulin and Ki67 (upper panels) or for insulin and BrdU (lower panel) are indicated by the arrowheads.

Supplementary figure 2



Supplementary Fig.2. Confirmation of the downregulation of the selected genes in dispersed P10 islet cells and INS832/13 cells. Dissociated islet cells from P10 rats (a, b) and INS832/13 cells (c) were transfected for two days with a siRNA against GFP (control), E2F1 (a), H19 (b) or Ago2 (c). The expression of each gene was measured by qRT-PCR, normalized to that of Hprt1 (a), 18s (b) or actin β (c) and is presented in fold change over the respective controls. The results are means \pm SEM of four (b,c) or five (a) independent experiments. Statistical differences were calculated by Student's t-test: *p<0.05, **p<0.01.

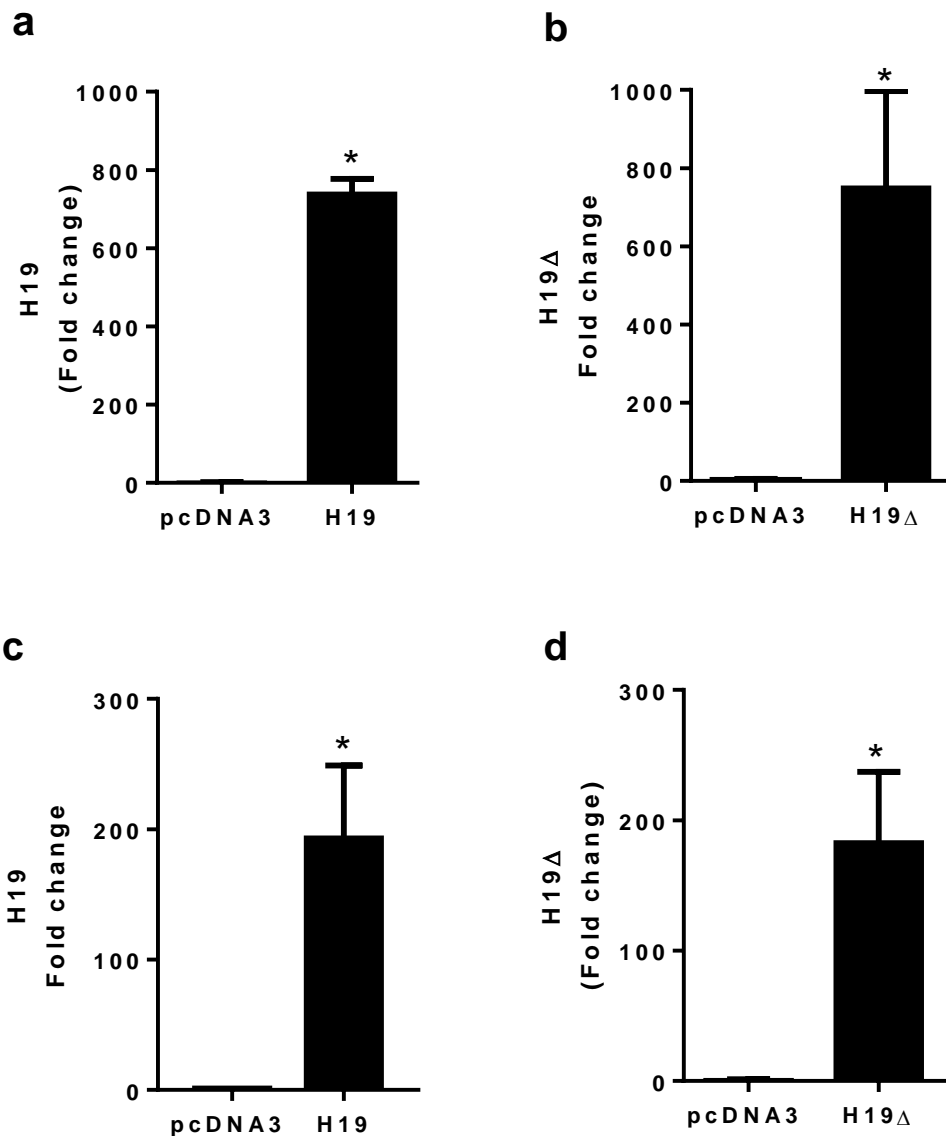
Supplementary figure 3



Supplementary Fig.3. c-Myc does not control H19 expression in newborn rat islets.

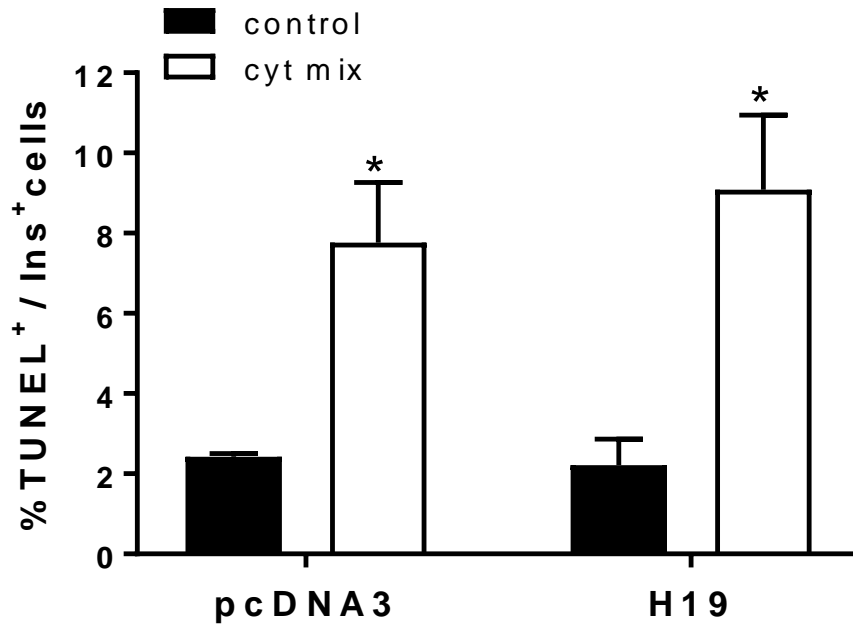
a) c-Myc expression was measured by qRT-PCR in the islets of P10 and adult rats ($n=3$). **b,c)** Dissociated islet cells from five day old rats were transfected with a control siRNA or with an siRNA against c-Myc for 72 hours. The expression of c-Myc (**b**) and H19 (**c**) was measured by qRT-PCR, normalized to Ppia and expressed in fold changes over control. The results are the mean \pm SEM of four (**b**) or three (**c**) independent experiments. Statistical differences were determined by Student's t-test. * $p<0.05$; ** $p<0.01$.

Supplementary figure 4



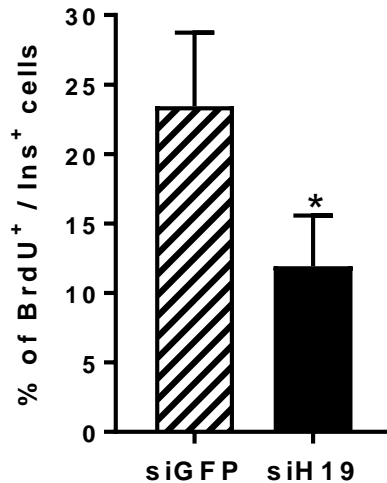
Supplementary Fig.4. Confirmation of upregulation of the indicated transcripts in INS832/13 cells and dispersed rat islet cells. INS832/13 cells (a,b) and dissociated islet cells from adult rats (c,d) were transfected for two days with an empty plasmid (pcDNA3) or a plasmid allowing the expression of H19 or a H19 mutant lacking the let-7 binding sites (H19Δ). The expression of each transcript was measured by qRT-PCR, normalized to that of Gapdh and expressed in fold change. The results are means \pm SEM of three (a,b) to four (c,d) independent experiments. Statistical differences were calculated by Student's t-test: *p<0.05.

Supplementary figure 5



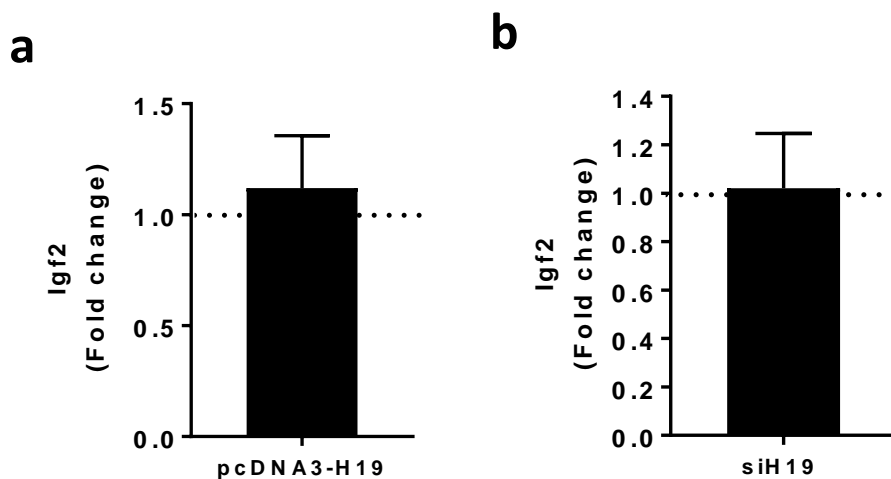
Supplementary Fig.5. Effect of H19 overexpression on apoptosis. INS832/13 cells were transfected for 48 hours with a control plasmid (pcDNA3) or a plasmid expressing H19. The cells were incubated with or without a mix of pro-inflammatory cytokines (TNF α ; IL1- β and IFN γ) for 24 hours. Cell death was assessed by TUNEL assay. The results are the means \pm SEM of three independent experiments. Statistical differences from control conditions were assessed by ANOVA analysis with Dunnett's post-hoc. * $p < 0.05$.

Supplementary figure 6



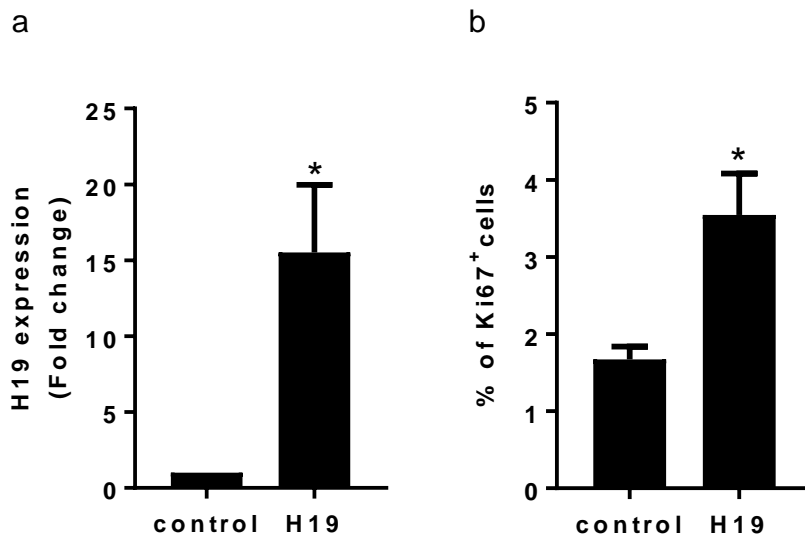
Supplementary Fig.6. Confirmation of the effect of H19 silencing on neonatal β -cell proliferation. Dissociated islet cells from 10 days old rats were transfected with a siRNA against GFP (control) or H19 and were incubated with BrdU for 48 hours. The fraction of proliferating insulin-expressing cells was assessed by scoring the cells double positive for insulin and BrdU. The data correspond to the mean \pm SEM of three independent experiments. Statistical difference from control condition was determined by Student's t-test. * $p < 0.05$.

Supplementary figure 7



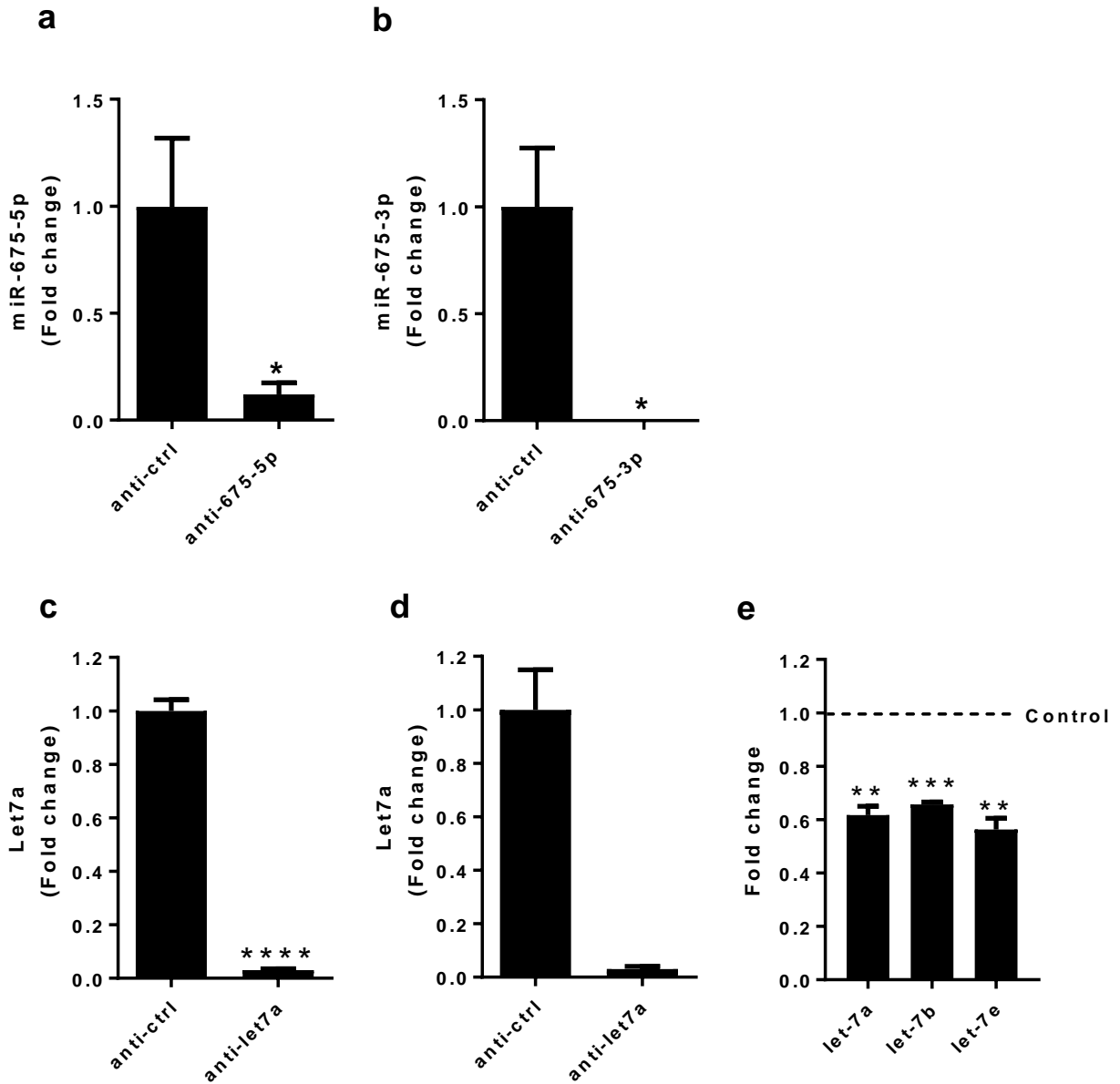
Supplementary Fig.7. Expression of Igf2 after modulation of H19 levels. (a) INS832/13 cells were transfected for 48 hours with a control plasmid or a plasmid allowing the overexpression of H19. **(b)** Dispersed islet cells from P10 rats were transfected with a siRNA against GFP or against H19. The expression of Igf2 was measured by qRT-PCR, normalized to those of Gapdh (a) or Ppia (b). The level of Igf2 under control conditions was set to one and is indicated by the dotted line. The results are means \pm SEM of two (b) to three (a) independent experiments. Statistical differences from control conditions were assessed by Student's t-test.

Supplementary figure 8



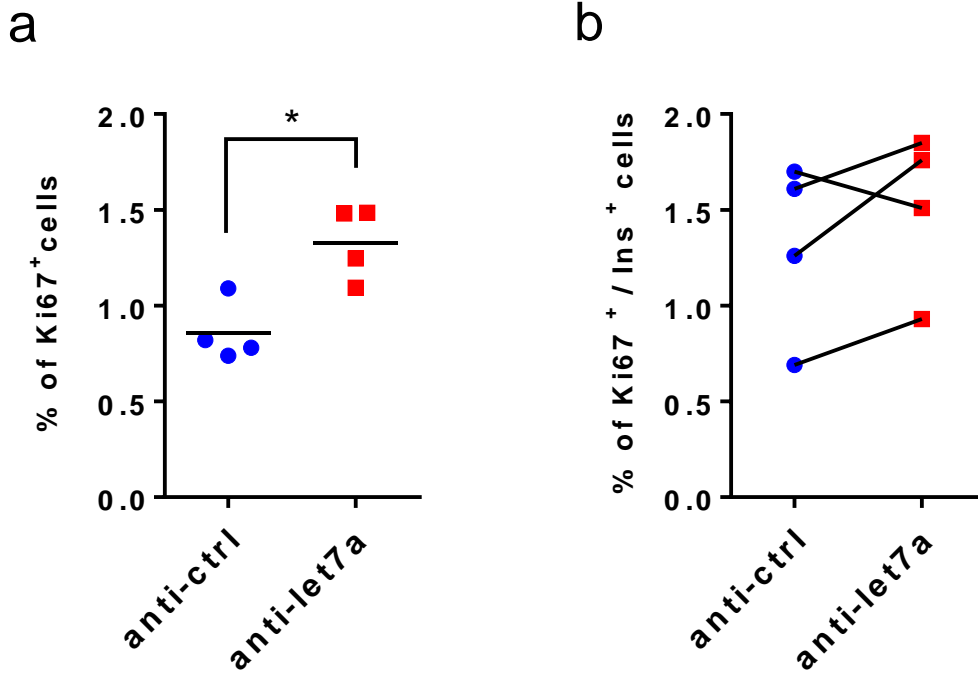
Supplementary Fig.8. Effect of H19 on human β -cell proliferation. Human 1.1 B4 cells were transfected with a control plasmid or a plasmid allowing the overexpression of human H19 for 48 hours. **(a)** The expression of H19 was measured by qRT-PCR, normalized to that of Hprt1 and expressed in fold change. **(b)** The fraction of proliferating cells was assessed by scoring Ki67 positive cells. The data correspond to the means \pm SEM of three (a) or four (b) independent experiments. Statistical differences from control conditions were determined by Student's t-test. * $p < 0.05$.

Supplementary figure 9



Supplementary Fig.9. Confirmation of the downregulation of selected miRNAs in INS832/13 and rat islet cells. Dissociated islet cells from P5 rats (a,b), adult rats (d,e) and INS832/13 cells (c) were transfected with a control anti-miR (anti-control) or with anti-miR directed against miR-675-5p (a), miR-675-3p (b), let-7a (c,d) or all let-7 family members (e). The expression of each miRNA was measured by real-time PCR and expressed in fold change. The results are means of two (d), three (b,c,e) or four (a) independent experiments and statistical differences were calculated by Student's t-test: * $p < 0.05$, ** $p < 0.01$, *** $P < 0.001$, **** $p < 0.0001$.

Supplementary figure 10



Supplementary Fig.10. Effect of a specific inhibitor of anti-Let-7a on β -cell proliferation. INS832/13 **(a)** and dissociated adult rat islet cells **(b)** were transfected with a control inhibitor or with an anti-miR specifically blocking let-7a. Two days later, the fraction of proliferating insulin-expressing cells was assessed by scoring Ki67 positive cells. Statistical differences from control conditions were assessed by Student's t-test. * $p < 0.05$

Supplementary figure 11

<p>TARGET: rat H19 length: 2677 MIRNA : rno-let-7a-5p length: 22</p> <p>mfe: -25.1 kcal/mol p-value: undefined</p> <p>position 639 target 5' A G C 3' GACUG AG CUGCUGCCUC UUGAU UU GAUGAUGGAG</p> <p>miRNA 3' AUG G U 5'</p>	<p>TARGET: rat H19 length: 2677 MIRNA : rno-let-7e-5p length: 22</p> <p>mfe: -25.3 kcal/mol p-value: undefined</p> <p>position 1927 target 5' U CACUCAGAACCCAC A G 3' GCUG UAC ACU CCUGCCUCA UGAU AUG UGG GGAUGGAGU</p> <p>miRNA 3' U U A 5'</p>
<p>TARGET: rat H19 length: 2677 MIRNA : rno-let-7b-5p length: 22</p> <p>mfe: -29.3 kcal/mol p-value: undefined</p> <p>position 1938 target 5' G U A C G 3' AACCAC AC CUA CUGCCUCA UUGGUG UG GAU GAUGGAGU</p> <p>miRNA 3' UGU 5'</p>	<p>TARGET: rat H19 length: 2677 MIRNA : rno-let-7f-5p length: 22</p> <p>mfe: -23.8 kcal/mol p-value: undefined</p> <p>position 639 target 5' A AGG C 3' GACUG CUGCUGCCUC UUGAU GAUGAUGGAG</p> <p>miRNA 3' AUGUUA U 5'</p>
<p>TARGET: rat H19 length: 2677 MIRNA : rno-let-7c-5p length: 22</p> <p>mfe: -27.4 kcal/mol p-value: undefined</p> <p>position 2527 target 5' U AG C 3' GGCCGUGC GCUUG GCCUCA UUGGUUUG UGGAU UGGAGU</p> <p>miRNA 3' U GA 5'</p>	<p>TARGET: rat H19 length: 2677 MIRNA : rno-let-7i-5p length: 22</p> <p>mfe: -29.2 kcal/mol p-value: undefined</p> <p>position 638 target 5' A A UG C 3' AG C AGGCUGCUGCCUC UC G UUUGAUGAUGGAG</p> <p>miRNA 3' UUG UG U 5'</p>
<p>TARGET: rat H19 length: 2677 MIRNA : rno-let-7d-5p length: 22</p> <p>mfe: -28.2 kcal/mol p-value: undefined</p> <p>position 1997 target 5' C CG A CUCC C 3' AGCU GC AGCCUACU CCUC UUGA CG UUGGAUGA GGAG</p> <p>miRNA 3' UA U A 5'</p>	

Supplementary Fig.11. Main potential binding sites for let-7 present in the rat H19 sequence. Representative binding sites for seven let-7 isoforms. Red letters show the seed sequence of let-7.

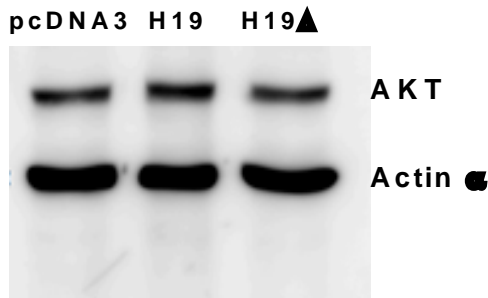
Supplementary figure 12

GGGGTGGGGGTAATGGGGAAACTGGGGAAAGATGGGAGTGTGGAGGAGAGTTGTGGGGTCCGAGGAGCACCTCGG
CATCTGGAGTCTGGCAGGAGTGTGAAGGACTGAGGGGCTAGCTCGGGCAGGGCAAAGGCAGCAGGACCTGGGAGG
AAGGAGCATGGTGTGGTTCACAGGCATTCAGAGGCTGGAAAACATCGGTGTGGGGTGAAGGGCCTGAGCTAGGG
TTGGAGAGGAACGGGGAGCCAGACATTCATCCCGGTCACTTTTGGTTACAGGACGTGGCGGCTGGTCCGATACAGG
GGAGCTGCTGGGAAGGGTTCGACCCCAGACCTGGGCAGTGAAGGTGTAGCTGGCAGCGGTGGGCAGGTGAGGACCG
CCGTCTGCTGGGCAGGTGAGTCTCCTTCTCTCTCTTGGCCCTCGCTGCACCTGACCTTCTAAAAGGTTTAGAGAGCG
AGGCCGCTGAGAAGAAGCAGCTGACCTCCCAACAGAATGGCACATAGAAAGGCAGGACAGTTAGCAAAGGAGACAT
CGTCTCGGGGGGAGCCGAGACAGAACAAGGCTGGGGGACCATTGGGCACCCCGGAGTGGAAAGAGCTTTTAGAGAG
AAGATAGAAGAGGTGCAGGGCTGCCAGTCAAGACTGAGGCCTGAGGCAAGTGATAGGAGGCCTTGGAGA
CAGTGGCAGAGACTATGGGATCCAGCAAGAGCAGAAGCATTTCTAGGCTGGGGTCAAACAGGGCAAGATGGGGGTCA
CAGGACACAGATGGGTCCCCAGCCGCCACCACATCCCACCCACCGTAATTCATTTAGAAGCAGGTTCAAGAGTGGC
TCTGGCAGGGCCTTCTGAGGCCTTTGCCAGAGCTTCGATGGCCGGAGAACGGGAAAGAAGGGCAGTGCAGGGTGT
AACAGGAAGGGAAACGGGGGCTGCAGGTATCGGACTCCAGAGGGATTTTACAGCAAGGAGGCTGCAGTGGGTCCAGC
CTGCAGACACACCATTCCCATGAGGCACTGCGGCCAGGGACTGGTGCAGAAAGGGCCACAGTGGACTTGGTGC
CTGTATGCCCTAACCGCTCAGTCCCTGGGTCTGGCATGACAGACAGAACATTTCCAGGGGAGTCAAGGGCACAGGA
TGAAGCCAGACAAGGCAGGCAGGTGGGGCAGAATGAATGAGCTTTCTAGGGAGGGAGGTTGGGTGCAGGTAGAGC
GAGGTAAAGCAGCTGGGGTGGTGGCCAGCGAGGCACCTGGCCCTCCAGAGTCCGTGGCCAAGGAGGGCCTTGC
GGCAGCGGAGCAGTGATCGGTGTCTCGGAGAGCTCGGACTGGAGACTAGGCCAGGTCTCTAGCAGAAGTGGATGTG
CCTGCCAGTCACTGAAGGCGAGGATGACAGGTGTGGTCAACGTGATAGAAAGACATGACATGGTCCGGTGTGATGG
AGAGGACAGAAGGACAGTCAATCCAGCCTTCCCTGAACACCGTGGGCTGGTGCCTGGGACACTGCCGTAGAAGCCGT
CTGTTCTTTTCCCTTTGCCCAAAGAGCTAACACATCTCTGCTGCTCTCTGGATCCTCTTCCCATAACAATTGAACCT
CAAGATGAAAGAAATGGTGTACCCAGCTCATGTCTGGGCCTTTGAATCCGGGACTTCTTTAAGTCCGTCTAGTT
CTGAATCAAGAATATGCTGCACTCAGAACACTACACTACTGCTCAAGGAATCGGCTCGAAGGTAAAGCTGAAGGA
ACAGACGGTGACAACATCTTGAAGAGCAGACCCACACAGCACCCACCCACCCCTGAGACTCCATCTTCATGGCCA
ACTAACTCTGCCTGGCCCGGGAGACCACCACCCACATCATCTGGAGCCAAGCCTCTAGCCCGGGATGACTTCATC
ATCTCCCTCCTGTCTTTTTTCTTCTTCTTCTTCTTCTGTAACCTVTTTTCTTCTTCTTCTTCTTCTTCTTCTGCTTGG
AGACTCAAAGCATCCGTGACTCTGCTCCCCACTCACCCCTTTTGAATTTGCACTAAGTGCATTGCACTGGTTTTGG
AGTCCCGGAGATAGCCTGAGTCTCTCCGTATGGATGTATACAGCGAGTGTGTAGGCCCTTTGGCTATGCTGCCCC
AGTGCCCGCCCGTCATCCACTTCTGTCTGAGGGCAACTGGGTGTGGCCGTGCGCTTGGAGGCTCACCTTCCCCTTG
CCTAGTCTGGAAGCAGTTCATCATAAAGTGTCAACGCACCTTCTTTCATCCTTTGTCCCTCCTCACCCAGGCT
CAACCAGAGTCTGGGTCCACCAATAAATACAGTTACAGTCAAAAAAAAAAAAAAAAAAAAAAAAAAAAAAAAAAAAA
AAAAAAAAA

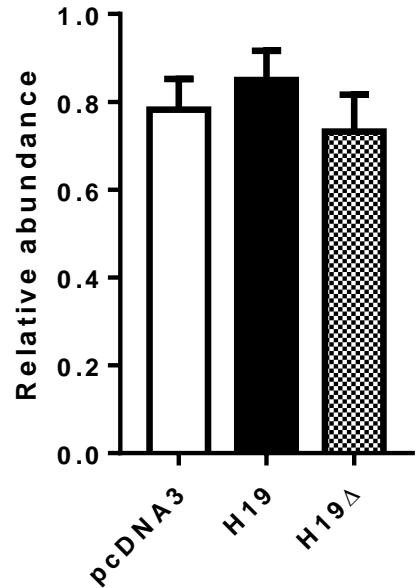
Supplementary Fig.12. Predicted let-7 binding sites present in H19. The green sequence indicates the binding site for let-7a, let-7d, let-7f and let-7i; and the blue sequence that for let-7b, let-7c and let-7e. Other possible let-7 binding sites in the H19 sequence are shown in red. The H19 Δ mutant lacks the green and blue sequences.

Supplementary figure 13

a

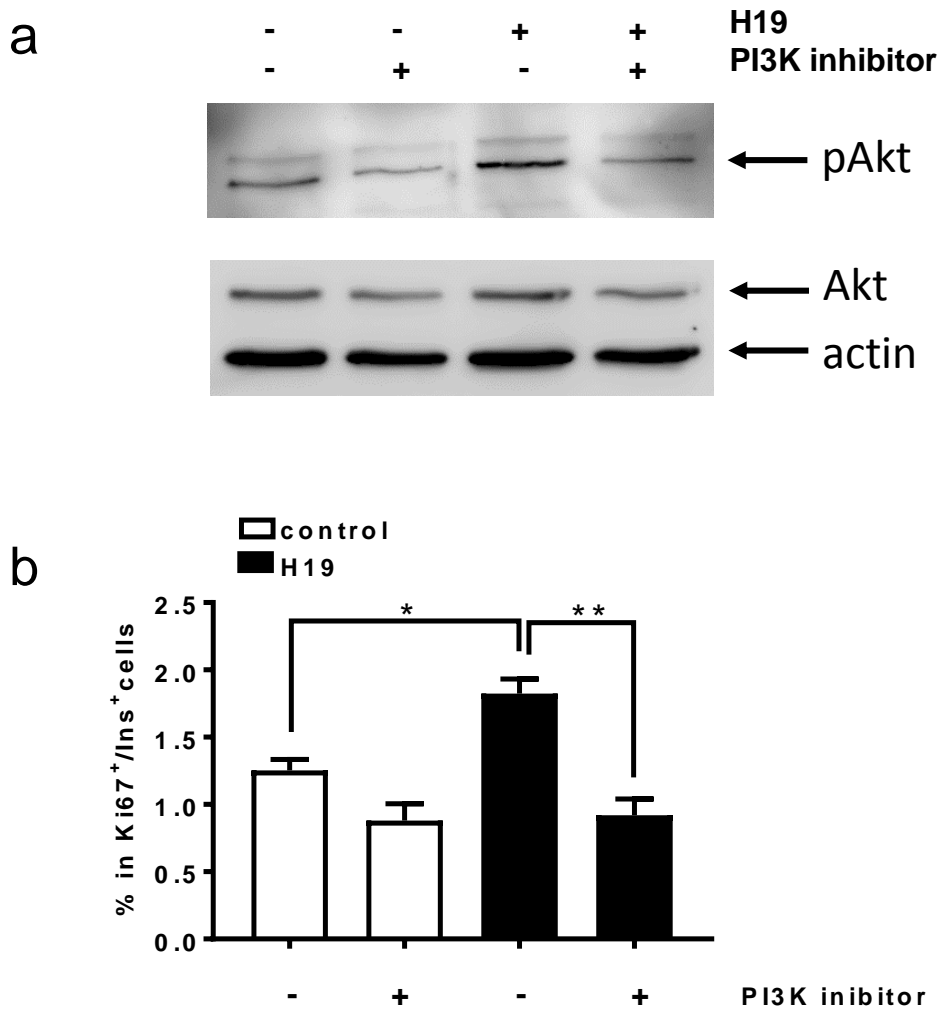


b



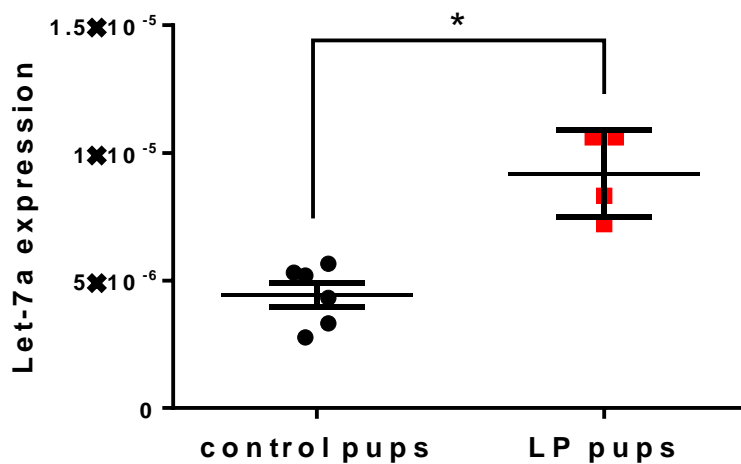
Supplementary Fig.13. Akt protein level after overexpression of H19 or of the H19 Δ mutant. (a) Representative western blot of Akt protein in INS832/13 cells transfected with a control plasmid (pcDNA3), a plasmid overexpressing H19 or the H19 mutant lacking the two main binding sites for let-7 (H19 Δ). (b) The intensity of Western blot bands of Akt were determined by densitometric scanning and were normalized to that of actin α . The results are means \pm SEM of four independent experiments.

Supplementary figure 14



Supplementary Fig.14. The proliferative effect of H19 necessitates the activation of PI3K. INS832/13 cells were transfected with a control plasmid (pcDNA3) or a plasmid overexpressing H19. PI3K activity was or not inhibited during 36 hours with 20 μ M of the PI3K inhibitor (LY294002). Phosphorylation at Thr-308 of Akt (a downstream target of PI3K) was assessed by western blotting **(a)**. The fraction of proliferating cells was assessed by scoring Ki67 positive cells **(b)**. The data correspond to the means \pm SEM of three independent experiments. Statistical differences from control conditions were assessed by one-way ANOVA with a Tukey'a post-hoc test. * p <0.05, **<0.01.

Supplementary figure 15



Supplementary Fig. 15. Expression of let-7a in the islets of the offspring from dams on a low-protein diet during gestation. Let-7a levels were measured by qRT-PCR in P10 control rats (control pups) and in P10 rats from dams on a low-protein diet during gestation and lactation (LP pups). The results are expressed as 2^{-ct} values and are the means \pm SEM of 4 and 6 animals. Statistical differences from control pups were calculated by Student's t-test: * $p < 0.05$.